Review

The Role of Liquid Crystal Elastomers in Pioneering Biological Applications

Faeze Shiralipour [1,2,3], Yeganeh Nik Akhtar [1,2,3,†], Ashley Gilmor [1,4,†], Gisele Pegorin [1,4,†], Abraham Valerio-Aguilar [1,4,†] and Elda Hegmann [1,2,3,4,5,6,*]

1 Advanced Materials and Liquid Crystal Institute, Kent State University (KSU), Kent, OH 44240, USA; fshirali@kent.edu (F.S.); ynikakht@kent.edu (Y.N.A.); asumme20@kent.edu (A.G.); gpegorin@kent.edu (G.P.); avaleri2@kent.edu (A.V.-A.)
2 Cell Biology and Molecular Genetics Graduate Program, Kent State University (KSU), Kent, OH 44240, USA
3 Department of Biological Sciences, Kent State University (KSU), Kent, OH 44240, USA
4 Materials Science Graduate Program, Kent State University (KSU), Kent, OH 44240, USA
5 Biomedical Sciences Program, Kent State University (KSU), Kent, OH 44240, USA
6 Brain Health Research Institute, Kent State University (KSU), Kent, OH 44240, USA
* Correspondence: ehegmann@kent.edu
† These authors contributed equally to this work.

Abstract: Liquid crystal elastomers have shown an attractive potential for various biological applications due to their unique combination of mechanical flexibility and responsiveness to external stimuli. In this review, we will focus on a few examples of LCEs used with specific applications for biological/biomedical/environmental systems. So far, areas of innovation have been concentrating on the integration of LCEs to enhance stability under physiological conditions, ensure precise integration with biological systems, and address challenges related to optical properties and spatial control of deformation. However, several challenges and limitations must still be addressed to fully realize their potential in biomedical and environmental fields, and future research should focus on continuing to improve biocompatibility, response to the environment and chemical cues, mechanical properties, ensuring long-term stability, and establishing cost-effective production processes. So far, 3D/4D printing appears as a great promise to develop materials of high complexity, almost any shape, and high production output. However, researchers need to find ways to reduce synthesis costs to ensure that LCEs are developed using cost-effective production methods at a scale necessary for their specific applications' needs.

Keywords: liquid crystals; liquid crystal elastomers; 3D printing; anisotropy; advanced manufacturing; additive manufacturing; orientational order

1. Introduction

1.1. Overview of Liquid Crystal Elastomers

At the time Otto Lehmann and Friedrich Reinitizer [1,2] encountered a double melting phenomenon in 1888 that will be described as a fourth state of matter (or liquid crystals, LCs), they did not realize the impact that their discovery would have on future technological applications. However, Lehmann visualized a technological application when, in 1909 [3], he suggested that some LCs can potentially act as artificial muscular driving motors. Subsequently, de Gennes in 1997 [4,5] supported this notion and a myriad of liquid crystal elastomer (LCE) applications have since been acknowledged. Most of these applications were related to properties combining orientational anisotropy of LCs with known elasticity of elastomers, and LCEs came to be known as materials capable of reversible actuation [6]. While the first discovery of LCs was related to the study of cholesteryl benzoate and related biological compounds, the main LC applications were heavily focused on liquid crystal displays (LCDs). LCDs were centered on the optical properties of LCs in the

presence/absence of an electric field. Since the last two decades, most of the new LCE applications have been back to their "roots" and target towards biological/biomedical applications, tissue engineering (TE), advanced manufacturing (AM), and soft robotics [7–9]. In this review, we aim to summarize most of the latest LCE's biological applications.

1.2. LCE Significance in Biological Applications

LCs exist abundantly in living systems, and many of them are found as lyotropic liquid-crystalline (LLC) phases and are a base for studying biomimetic chemistry. LLCs are predominantly found in cell membranes, mainly made of phospholipids [10]. Silk is another example of LCs; the organization of the proteins that form silk presents a liquid crystal phase [11,12]. DNA can also form liquid crystal phases [13]. During two-dimensional (2D) cell culture experiments, LC behavior has been observed where cells form topological defects. These topological defects have shown certain biological effects that can induce cell extrusion and potentially cell death [14]. Tissue Engineering (TE) combines the knowledge of both biology and engineering with the determination of finding ideal alternatives to restore or regenerate ailing or impaired tissue [15], and most of those alternatives focus on three-dimensional (3D) systems looking for better outcomes than those found in 2D systems [16,17]. Most of these 3D systems need to overcome most commonly found limitations, such as being non-toxic, providing effective support for cells and forming tissue, promoting extracellular matrix, sustaining 3D cell growth, and having appropriate mechanical properties similar to those tissues of interest [18–22].

LCEs combine the orientational anisotropy of LCs with the intrinsic elasticity of elastomers and have been recognized as ideal materials capable of reversible actuation [23,24]. Biological/biomedical applications of LCEs as part of TE have become an important part of current academic research as responsive and anisotropic 3D cell scaffolds. Within the last decade, AM, or 3D printing, with its layer-by-layer fabrication process, has allowed the creation of complex 3D structures with high reproducibility in endogenous environments. For 3D printing, the use of synthetic-based bio-inks has been used, showing good cellular responses, biocompatibility, and capability of ECM formation [25,26]. Figure 1 shows an example where LCE scaffolds are suitable for most types of somatic and immortal cells. LCEs have been shown to be ideal substrates for cell proliferation, differentiation, and maturation, as well as serving as an ideal host for primary cell development and for in vitro studies of myelination. Figure 1 shows a study conducted in a 3D environment that promoted ECM formation and maturation processes of co-cultured neuroblastomas (SH-SY5Y) and human oligodendrocyte cells (MO3.13). Indicating that LCE scaffolds can impact cellular function, differentiation, and other cell processes, enabling the mimicry of an endogenous environment for long-term studies.

At the beginning, many LCEs included polycaprolactone (PCL) and polyethylene glycol (PEG)-based inks. LCE-inks have been reported, for example, as nematic-based thermally responsive LCE ink [27], as direct-write printed into 3D structures, or as high operating temperature direct ink writing (HOT-DIW) [28]. It is important to note that processing can increase the likelihood of external stimulation of LCE shape actuation [29]. Much has changed since the first LCE reports, where now LCE actuators are no longer only thin film devices; they can now be complex 3D structures. LCE 3D printing formulations are constantly improving, allowing the development of thermal- or photo-crosslinked LCEs and increasing a wide range of printing possibilities [30–34].

We are aware that each year we are faced with a fast-growing aging population that inevitably brings age-related diseases [15]. On top of that, accidents occur involving the loss of mobility, organ, and limb function. To combat this, the medical community relies extensively on prosthetic and rehabilitation devices to bring back mobility to injured people. Looking ahead, there has been a shift in focus onto soft robotics and medical robotics, for the purpose of finding better, individualized, more human-like alternatives, integrating novel sensors, actuators, and materials into prosthetics to help increase life expectancy and improve the quality of life of affected individuals. The main objective is to substi-

tute old technology that involved passive and at times skin-irritable materials [35,36] for flexible electronics and soft devices [37–39] that respond dynamically to external stimuli, including temperature, chemical cues, electricity, and light, promoting multifaceted applications [40]. Soft materials used in robots require different levels of biocompatibility, biomimicry, sensing, actuation, and computation/informatics [41]. Most importantly, there is a need for mechano-sensation electronics that can provide sensations of cold/hot, touch, pain, and comfort [42]. LCEs have been recently seen as soft responsive materials that can revolutionize the realm of soft robotics, leading to a new era of versatility and adaptability [43].
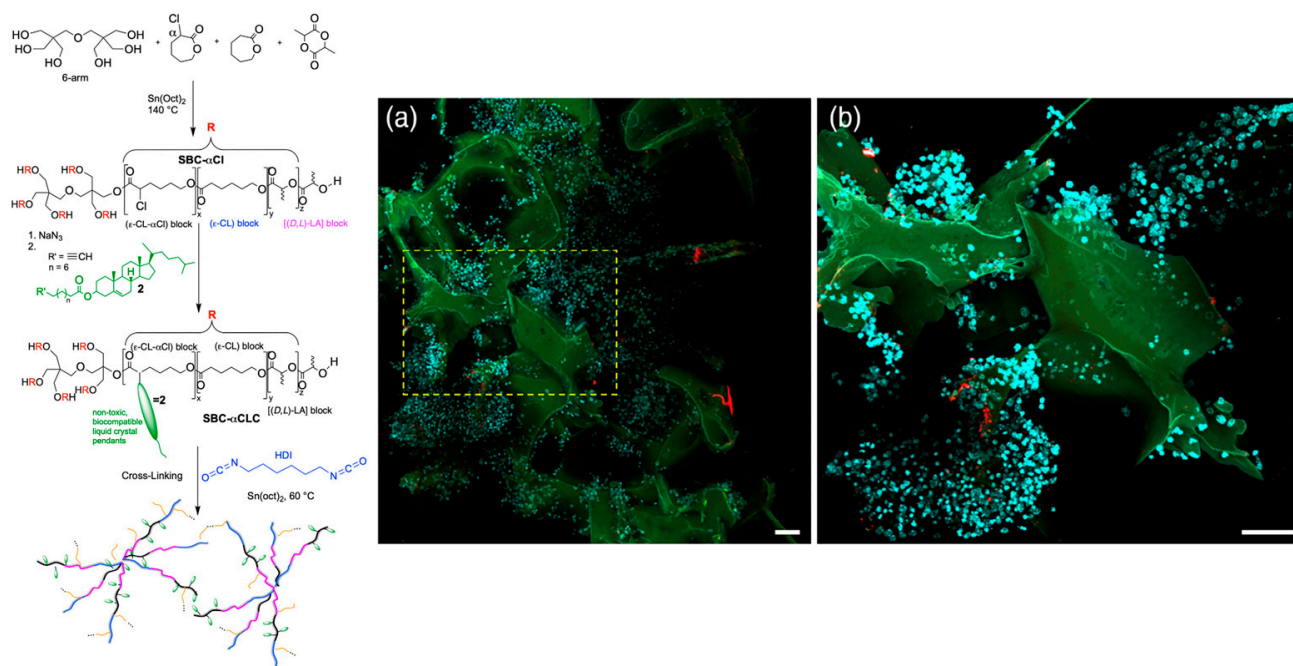
Figure 1. Example of liquid crystalline elastomers (LCEs). Scheme shows the synthetic pathway of a LCE star block-copolymer with cholesterol liquid crystal as pendant units and (**a**) confocal image of primary mouse brain cells grown on LCE scaffold and (**b**) enlarged image of selected area in yellow (cell nuclei stained in blue, scale is 60 μm). Reprinted from *J Appl Polym Sci* [25]. Copyright (2023) with permission from Wiley (Hoboken, NJ, USA).

2. Fundamentals of Liquid Crystal Elastomers

LCEs are unique materials that combine the properties of liquid crystals with elastomers, resulting in materials with distinct physical and chemical characteristics. LCEs consist of LC mesogens (rod-like molecules) that are incorporated into a crosslinked polymer network (see Figure 2) [44]. Mesogens can be attached to the polymer backbone (main-chain LCEs) or connected via flexible spacers (side-chain LCEs). LCEs can be either monodomain, where the mesogens are uniformly aligned throughout the material, or polydomain, where the alignment varies spatially. Monodomain LCEs exhibit more shape-changing abilities.
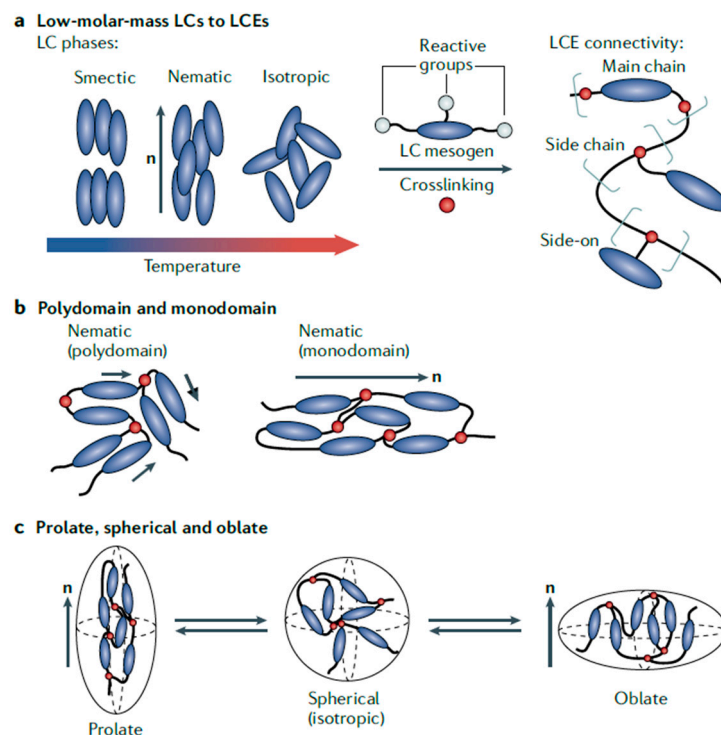
Figure 2. Types of liquid crystalline elastomers (LCEs). (**a**) The rod-like mesogens are connected via reactive functional groups in the main chain, end-on side chains, or side-on side chains. (**b**) Polydomain LCEs have local domains of nematic order, and monodomain LCEs have a common director throughout the network. (**c**) In a monodomain LCE, the chain configuration can be prolate or oblate, with a spherical configuration in the isotropic state. Reprinted from *Nat. Rev. Mat* [45]. Copyright (2021) with permission from Springer Nature (Berlin/Heidelberg, Germany).

2.1. Chemical and Physical Properties

LCs are composed of anisotropic molecules called mesogens, which can be rod-like (calamitic), disc-like (discotic), or lath-like (sanidic) in shape. These mesogens exhibit phase transitions based on temperature (thermotropic LCs) or concentration (lyotropic LCs), with the most common phases being nematic, smectic, and cholesteric. Mesogens can have various functional groups such as thiols, acrylates, or epoxies, which are crucial for their polymerization and cross-linking into LCEs. The stability of these phases is influenced by the chemical structure of the mesogens and the polymer backbone. For instance, side-chain LCEs [23,46] can show stable nematic or smectic phases over a wide temperature range (see Figure 2). The elastomeric properties of LCEs arise from crosslinking the polymer chains, either through covalent bonds or physical interactions. Crosslinking density can significantly impact the mechanical properties and thermal behavior of the LCEs [47]. The chemical structure and functionalization of mesogens affect their alignment within LCEs, which can be controlled using techniques such as mechanical stretching, surface alignment, field-assisted alignment, and shear alignment [45,48].

LCEs exhibit anisotropic mechanical properties due to the alignment of liquid crystal molecules within the elastomer matrix, allowing them to respond directionally to external stimuli like light. For instance, certain LCEs are designed to respond to light stimuli, particularly those containing azobenzene groups. Azobenzene can undergo a reversible transformation between its trans and cis isomers when exposed to UV light, resulting in a change in the molecular alignment [45,49].

They display rubber-like elasticity and can undergo significant deformation, with the presence of polymer networks and liquid crystalline molecules imparting them with soft and super-soft elasticity, making them suitable for applications like artificial muscles and actuators. The thermo-elastic properties of LCEs enable them to change shape in response to

temperature changes, particularly notable in side-chain liquid crystal elastomers (SC-LCEs), where different mesophases exhibit stability over a wide temperature range. Additionally, LCEs can remember and return to their original shape after deformation when exposed to certain stimuli, such as temperature changes or light, leveraging this shape-memory behavior in applications requiring precise and reversible actuation [45,49]. LCEs can be designed to respond to various chemical stimuli, which makes them useful in the development of sensors and responsive materials. This responsiveness is often achieved by incorporating photoresponsive or thermoresponsive groups within the polymer matrix [48].

2.2. Synthetic Strategies

There are different synthesis and alignment methods that lead to the production of LCEs with diverse molecular structures and properties. Several of these are displayed in Figure 3. The various approaches are described below and include the following:
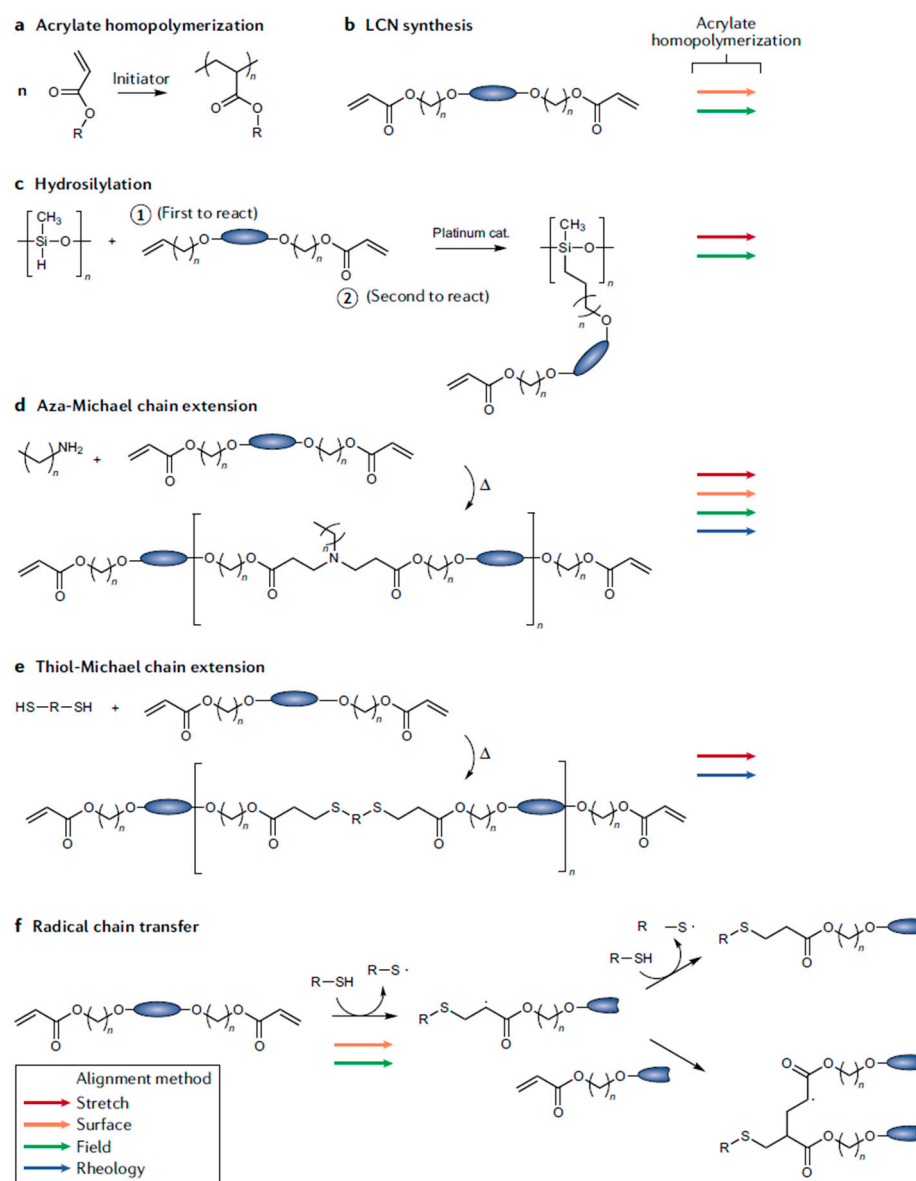
Figure 3. Synthetic strategies for crosslinking LC polymers and their corresponding alignment methods. Reprinted from *Nat. Rev. Mat* [45]. Copyright (2021) with permission from Springer Nature.

Mechanical alignment: This technique includes a two-phase reaction. Initially, the liquid crystal elastomer (LCE) mixtures undergo partial polymerization. They are then

mechanically stretched to align the polymer chains. While maintaining this stretched alignment, the polymerization process is completed, locking in the oriented structure [49].

The field-assisted alignment can be divided into two primary categories: (1) Electric field alignment uses electric fields to orient LC molecules by taking advantage of the molecules' uneven response to electric fields in different directions. (2) Magnetic field alignment utilizes magnetic fields to position liquid crystal molecules. It relies on the molecules' varying magnetic properties along different axes. Both techniques exploit the anisotropic nature of LC molecules to achieve alignment [50].

The 3D printing alignment technique uses the fluid dynamics inherent in 3D printing to orient LC molecules. As the material is pushed through a printer nozzle, it experiences forces that stretch and shear the material. The mechanical stress suffered during extrusion naturally causes the LC molecules to line up (or orient) in a preferred direction [51].

Chain extension reactions include three subcategories: (1) Aza-Michael Addition, which combines LC monomers containing two acrylate groups with primary amines. (2) Thiol-Michael addition involves reacting extra diacrylate LC monomers with thiols. (3) Thiol-Ene reactions involve a gradual polymer growth process, linking monomers with two thiol groups to LC monomers featuring diallyl ether functionalities. These reactions all serve to lengthen molecular chains, but each uses different chemical pathways and functional groups to achieve this goal [49,52].

Hydrosilylation is a two-step process where LC monomers and crosslinkers react with a linear polysiloxane in the presence of a platinum catalyst, followed by mechanical alignment and final polymerization [49].

The dynamic covalent chemistry method incorporates dynamic covalent bonds that can break and reform under stimuli. This technique allows alignment under load and subsequent retention of alignment after stimuli removal [53].

White et al. reported an extensive list of work related to LCEs, including finding ways to simplify the synthesis process and control the mechanical properties of the materials through thiol-acrylate and thiol-ene reactions [54–56].

3. LCEs in Biomedical Engineering

3.1. Drug Delivery Systems

The application of topical medications and remedies has been a method used throughout human history. Over the past several decades, transdermal drug delivery has been a growing field, often via adhesive patches applied to intact skin. An increasing number of medications are now available in a transdermal patch form, as this route can address issues related to other routes of drug administration, such as pain from injections, inconsistent serum medication levels, increased side effects, decreased bioavailability, and patient noncompliance [57].

One issue that presents with this approach to medication administration is the lack of ability to control the drug delivery in an "on/off" manner. While some patches can deliver drugs slowly over a period of time, none can adjust the delivery rate or stop the drug release altogether while the patch is still in place on the skin. To address this concern, Nozawa et al. immobilized a liquid crystal (LC) monooxyethylene trimethylolpropane (MTTS) between sheets of a hydrophobic, porous Celgard membrane. Their goal was to utilize the thermos-responsive properties of the thermotropic LC to control drug permeation through the membrane. Permeability of antipyretic and analgesic medications acetaminophen and ethenzamide and non-steroidal anti-inflammatory drugs indomethacin and ketoprofen was studied, both in vitro in diffusion cells and on excised rat skin and in vivo on the abdomens of rabbits. Testing was performed for temperatures of 32–38 °C, and for all medications tested, drug permeation through the membrane was reported to have been dependent on the temperature. For all drugs except ketoprofen, the reported "on/off" temperature was at the phase transition temperature of the liquid crystal, 38 °C; for ketoprofen, the permeation increased proportionally with the temperature, which they report is likely related to the ethanol in the solution. The results of this work indicate that incorporating LC in a drug

delivery system may be a way to control the drug release due to the transition between an ordered and isotropic system, where the pathways for the drug molecules to pass through the membrane are limited in the liquid crystalline state [58].

Along similar lines, Chen and colleagues embedded a liquid crystal cholesteryl oleyl carbonate (COC) into a nylon membrane to be tested for the penetration of the bronchodilator medication salbutamol sulfate. They found that the drug penetration correlated with the amount of LC in the membrane as well as with temperature change, as it was tested over the range of 10–25 °C. According to their results, the COC made the surface of the membrane hydrophobic, whereas salbutamol sulfate is hydrophilic, so it was not able to permeate through the hydrophobic membrane. However, at certain higher concentrations, drug penetration increased again, which they report could be due to aggregation of the COC on the surface, creating open channels through which the drug could travel. Therefore, drug penetration through their LC-embedded polymeric membrane was both rate-controlled and thermally responsive, further evidence that LC materials can be utilized to modulate the permeation of medications through a membrane. However, it is important to note that the phase transition temperature of the LC used in this study was not suitable for body temperature applications, and this would need to be addressed before it could be used for drug delivery [59].

This approach was further demonstrated by Inoue et al. with the development of thermoresponsive membranes containing a side-chain liquid crystal polymer (LCP) cast onto a polyvinylidene difluoride (PVDF) support membrane. It was found that the nematic-isotropic transition temperatures (T_{NI}) of the LCPs varied with the amount of mesogenic pendants added to the polymer chain, so that membranes could be designed to have T_{NI} at body temperature, addressing the issue of membrane performance at biologically relevant temperatures. In this work, permeation of the drugs indomethacin and vitamin B_{12} through the LCP/PVDF membranes was tested and found to be inhibited in the nematic phase but substantially increased in the isotropic phase (Figure 4) [60].
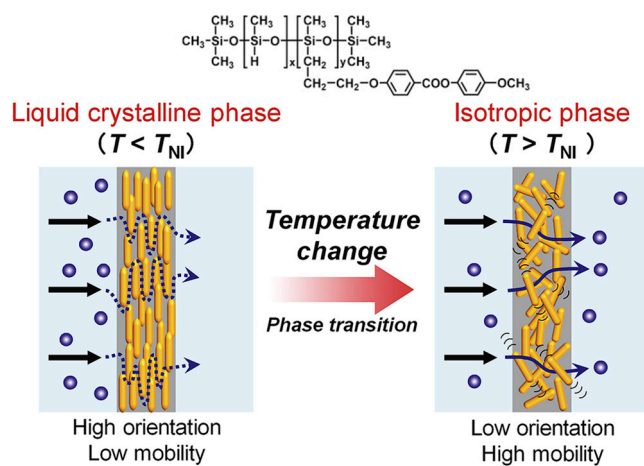
Figure 4. Mechanism for drug permeation through a thermoresponsive membrane composed of liquid crystal polymer (LCP) and polyvinylidene difluoride (PVDF). At temperatures below the nematic-isotropic (NI) transition temperature, the molecular arrangement of the nematic state prevents the drug from passing through the membrane. In the isotropic state above the transition temperature, the drug molecules may pass through. Reprinted from *J Membrane Science* [58]. Copyright (2019) with permission from Elsevier (Amsterdam, The Netherlands).

The aforementioned studies have utilized thermotropic LC materials within other polymers to act as physical barriers to the permeation of drug molecules rather than to encapsulate and release the drug itself. In contrast, Stepulane and collaborators developed a method of loading and delivering medications in a lyotropic liquid crystal elastomer (LLCE). LLCEs were composed of polydimethylsiloxane (PDMS), triblock copolymer di-

acrylated Pluronic F127 (DA-F127), and water in various ratios, resulting in four different LCE samples with different mechanical properties. The samples were polymerized into thin sheets for characterization and experimental procedures. Two drugs were tested to determine the ability of the LCEs to load and deliver a polar medication, Vancomycin, and a nonpolar medication, Ibuprofen. Both the drug loading and subsequent elution were performed in solution using small pieces of each LCE that were punched out from the polymerized sheets. Elution was monitored and measured via UV spectrometry at specific time intervals until no more drug release was noted (Figure 5). It is reported that two of the four LLCEs delivered a high amount of Vancomycin over a period of 6–7 days, likely related to their higher PDMS content that contributes to a strong network of crosslinks in the elastomer. The results were similar to the release of Ibuprofen, but it was noted that the release of Ibuprofen had a steadier release rate, as it is found inside the micelles due to its hydrophobicity. In this work, the researchers were able to show that an LLCE system can be utilized for the delivery of both hydrophobic and hydrophilic drugs, although the ideal composition of the LCE for each drug may need to be determined [61].
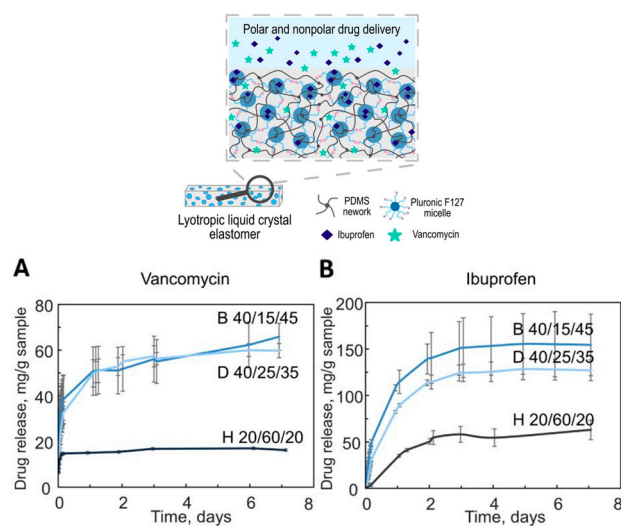
Figure 5. Drug release from lyotropic LCEs of (**A**) vancomycin in Milli-Q water and (**B**) ibuprofen in 1 wt% SDS buffer. Samples composed of polydimethylsiloxane (PDMS), triblock copolymer diacrylated Pluronic F127 (DA-F127), and water in the following ratios: B (40–15–45 wt%), D (40–25–35 wt%), and H (20–60–20 wt%). Reprinted from *Colloid Surface B* [59]. Copyright (2023) with permission from Elsevier.

Thermotropic LC materials have been shown to make drug delivery systems more tunable by the ability to control permeation, and lyotropic LCEs offer an attractive method of encapsulating and releasing drugs over a sustained period. Investigation into this application of LCEs has been limited; however, the results of these previous works should encourage more researchers to pursue this area further and develop practical methods of using LCEs for real drug delivery systems.

3.2. Soft Robotics

Soft robotics often refers to Shape Memory Polymers (SMP) that are flexible, sensitive, and possess good mechanical properties. Ideally, the material should be able to respond to external stimuli such as bending, stretching, twisting, and compression. The search for a material that reacts and works as an organic muscle fiber is an ongoing field with many branches working for the same goal. Since 1969, with the prediction of Pierre deGennes and the subsequent synthesis of the first perfect monodomain nematic elastomer by Küpper and Heino Finkelmann in 1991 [62], LCEs have been sought to be a great solution for muscle-like material. They showed three important characteristics: orientational order in amorphous soft materials, responsive molecular shape, and quenched topological constraints.

One of the biggest downsides for the utilization of LCEs in the soft robotic field is the low mechanical properties. For a natural muscle, the work capacity can reach 40 J kg^{-1} with a maximum strain over 40% [63]. A synthetic LCE shows potentially closer values but at times is not enough. Many efforts have been made in the field to increase the strain and work capacity exerted by the materials. One of the strategies is to dope the LCE with conducting materials. Rigid dopants like Carbon Nanotubes (CNTs) are embedded as sheets, forming a multilayer structure in combination with the LCE [64] and were reported to increase the strain and work capacity in response to an applied voltage. Another example is liquid dopants, which are getting attention since liquid dopants do not interfere with the mobility or flexibility of the LCE. The liquid dopant is mixed in the solution of the LCE as dispersed droplets of eutectic gallium indium alloy (EGaIn), which facilitates the synthesis process [65].

Applications of these kinds of materials have not often been considered in the field of biology. Only lately, the TE field has been looking at the implementation of soft robots made of LCEs as scaffolding for cell culture. A clear example of this surge of applications for the LCE soft robots are all the "bio-inspired" actuators. Among these examples, we can mention the "Janus" soft robot composed of two layers that can undergo opposite deformations simultaneously, emulating the grip of a hand or, depending on the complexity of the 3D shape, even mimic the movement of a starfish [66]. The very popular azo-dies do not escape from the TE field; many efforts have been directed to improve the photo-mechanical effect deriving from the change in morphology during the trans-cis isomerization of these molecules in efforts to have a viable artificial muscle-like material [67]. But the area of interest is much larger than just artificial muscles. In the last few years, we have seen light-driven soft robots that mimic caterpillars [68], with more complex modes of movement like rolling [69] with the ability of stirring and even swimming [70].

There are reports of thermotropic LCEs in combination with thermotropic dyes that not only change shape but also color [71] (Figure 6). These are called "chameleon-" or "octopus-like" biomimetic materials, developed with the goal of achieving some camouflage behavior in the soft robot. Finally, some LCE soft robots are created to heal or replace damaged tissue in the human body. Recent studies report a soft robot made of a LC membrane capable of secreting both polar and nonpolar liquids, similar to the human skin [72]. Generated digital models and 3D printed scaffolds of blood vessels give us a different perspective on how the tunability of physical characteristics in LCEs can mimic the human body and maybe be implanted and grafted for wound healing and tissue regeneration [34].
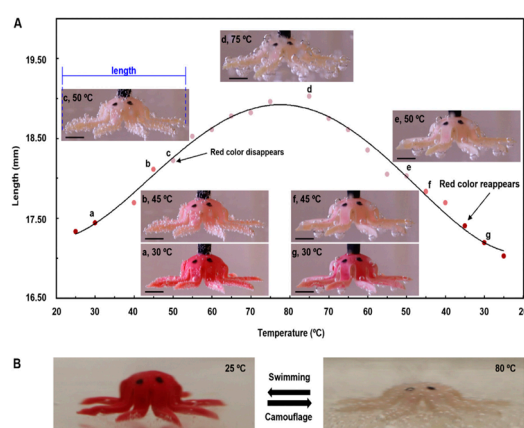
Figure 6. (**A**) Shape and color-changing thermochromic liquid crystal elastomer. Scale bar: 3 mm, (**B**) Octopus-like material mimicking the swimming/camouflage of the octopus in nature. Adapted with permission from Li et al. [69]. Permission conveyed through Copyright Clearance Center, Inc. (Danvers, MA, USA).

So far, advances in soft robotics research have focused on designing materials that are reactive, flexible, and robust. Research in the area of flexible electronics and tactile sensing has progressed greatly; this has been thankfully due to efforts in bringing together advances in many areas of materials research. Multidisciplinarity has been the key to advancing the research without sacrificing individual advances from the different fields. Future success will depend on the combination of flexible and stretchable mechanical properties of materials combined with sensors and possibly the ability to self-healing. The path is to continue to improve materials design and properties for better bio-inspired soft robotics, biomedical applications, and prosthetics.

3.3. Tissue Engineering

3.3.1. Cell Culture Platforms

Cells in vivo experience a variety of environmental conditions, including extra-cellular matrix (ECM) stiffness and elasticity, tensile forces, fluid viscosity and shear stress, and hydrostatic pressures. These features are a source of mechanical signals to the cells, which are then translated into biochemical signals by cellular mechanotransduction [73]. Much of this process occurs through focal adhesions, which are large complexes of proteins that connect the cytoskeleton inside the cell with the ECM outside the cell. These proteins undergo unfolding to expose binding sites, post-translational changes, or shuttling to the nucleus that trigger the activation of molecular pathways or mechanosensitive genes [74]. Studies have shown that cell behavior can be directed by altering the characteristics of the environment [75–77], such as patterning [78].

Babakhanova et al. developed a method to control the arrangement of microparticles by employing an LCE coating that undergoes a trans-to-cis isomerization when irradiated with UV light. To achieve this, LC cells were designed with unique patterns in mesogen arrangements such that, upon isomerization, the spatial topography inside the cell would transform, creating areas of lower potential energy at the desired locations. When spherical particles of resin were placed onto the LCE coating, the microparticles would be directed by gravity to these predesigned valleys. One main advantage of this method is the reversibility of the process: the LCE coating reverted completely back to its flat topography upon cis to trans isomerization under visible light. Although this method had not been used in biological applications, the authors noted that this type of device could prove useful in areas such as the control of cell behavior and targeted drug delivery [79]. Later on, they pursued an approach by making grooved substrates for cell cultures using smectic A LCE coating over polyimide molecules of planar alignment. This geometry caused areas of LC defects on the substrate, generating periodic grooves on the surface. For cell cultures, human dermal fibroblasts (hDFs) were used. Four substrates were tested: flat topology with and without fibronectin (FN), and grooved topology with and without FN.

Cells were seeded and cultured for seven days or until confluent, after which analysis revealed that the cells seeded on flat substrates were multinucleated, elongated, and had poor alignment (Figure 7). Whereas the grooved substrates with FN culture had a scalar order parameter of 0.66, and the grooved one with FN had the highest amount of cellular alignment with an order parameter of 0.81. The morphology of the cells on the grooved substrate without FN was highly elongated with an aspect ratio of 6.4, but those with FN were found with many actin filaments and filopodia and an aspect ratio of 3.2. From these results, the authors concluded that depositing the FN was not necessary to have the cells adhere, align, or migrate during the culture. However, it is clear that the nanogrooved topology greatly affected the cell proliferation and alignment [80].
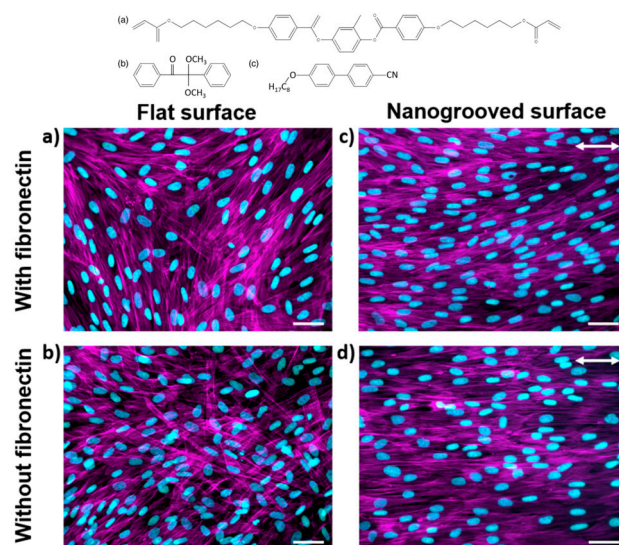
Figure 7. Fluorescent microscopy images of hDF grown on substrate (**a**) flat glass with fibronectin; (**b**) flat glass without fibronectin; (**c**) glass with nanogrooved SmA LCE coating and fibronectin; (**d**) glass with nanogrooved SmA LCE. Actin filaments stained with Alexa Fluor 488 phalloidin are presented in purple, while the cyan regions indicate the nuclei stained with DAPI. The arrows represent the direction of the nanogrooves. Scale bars 50 μm. Reprinted from *J Biomed Mater Res A* [78] Copyright (2020) with permission from Wiley.

Turiv and collaborators further studied the ability to control hDF behavior using an LCE substrate. In this case, plasmonic photoalignment was used to orient the molecules of the LCE precursor into the desired pattern, after which the photopolymerization reaction was used to secure this pattern. The specialized surface topography of the LCE formed when in contact with water, causing swelling of the LCE. In experiments, the authors showed that HDF cells grown on the LCE substrate aligned with the director, resulting in high scalar order parameters. Furthermore, the surface and number densities as well as phenotypes of the cells were affected. Positive topological charge defects were associated with an increased cell density and round shape, while negatively charged defects were found to have lower densities of cells and elongated shapes. Considering these results, the use of a photoaligned LCE may be a promising method of controlling cell proliferation, migration, and differentiation, as well as the possibility of developing environmentally responsive substrates that provide dynamic topographies for the cells [81].

3.3.2. Effects of Mechanical Properties of LCEs on Cell Behavior

LCEs' mechanical characteristics are extremely customizable, giving control over their stiffness, elasticity, and reaction to outside stimuli. Because of their ability to be customized, LCEs are especially appealing for use in dynamic cell culture conditions, where the mechanical characteristics of the cells are important factors influencing their behavior.

Agrawal et al. investigated the potential of monodomain LCEs for dynamic cell culture by making use of their reversible shape changes with heating cycles. Good adhesion and survivability were demonstrated by neonatal rat ventricular myocytes (NRVM) grown on LCE substrates. Because the LCEs could undergo cyclic uniaxial contraction and elongation, the cells were able to operate in a dynamic mechanical environment. Cell alignment, elongation, and differentiation are encouraged by this cyclic strain, which is like the physiological mechanical environment that cardiomyocytes encounter in vivo. It is important to note that the LCE surface was prepared for cell culture using methods like collagen coating, gold sputtering, and oxygen plasma cleaning. These alterations allowed the LCEs to function as dynamic substrates for cell culture while simultaneously enhancing cell adherence and preserving their mechanical characteristics [82].

In another study, Herrera-Posada et al. investigated magneto-responsive LCE nanocomposites enhanced with iron oxide nanoparticles. These LCEs could be remote-actuated due to their anisotropic, directed nematic structures reacting to magnetic fields. The nematic-to-isotropic phase transition temperature was decreased using nanoparticles, enabling actuation nearer physiological conditions. Higher nanoparticle concentrations enhanced the Young's modulus while decreasing the maximum thermomechanical deformations, according to tensile testing. Reversible deformations under alternating magnetic fields were shown in magneto mechanical tests; the degree of deformation depended on the concentration of particles. Under a 48 kA/m field, the maximum contraction for LCEs with 0.5 and 0.7 wt% particle loadings was approximately 24%, indicating their potential for use in dynamic substrate applications. Furthermore, by functionalizing the surfaces of these LCEs with collagen to facilitate NIH-3T3 fibroblast adhesion and proliferation, the study investigated the biocompatibility of these LCEs. Staining with fluorescence and confocal imaging verified strong cell adhesion and network development on the LCE substrates. According to their results, magneto-responsive LCEs with controlled deformation provide a viable means of establishing dynamic cell culture environments that replicate mechanical stimuli found in vivo, hence promoting tissue engineering and regenerative medicine applications [83].

Prévôt et al. investigated the mechanical properties and cellular behavior of smectic liquid crystal elastomers (LCEs), which are intended to be responsive scaffolds for tissue engineering. These LCE scaffolds offer mechanical properties that resemble different tissues, regulated degradability, and biocompatibility. Various LCE forms, such as films, foams, and microspheres, were investigated in this work to maximize pore size and shape for tissue growth and cell infiltration. Testing for mechanical properties demonstrated that these LCEs have a Young's modulus (YM) that ranges from 2 to 4 MPa, depending on the cross-linking density and structural arrangement. This means that these LCEs are appropriate for use in specific tissues, such as neurons. Studies on cell behavior concentrated on the adhesion, growth, and orientation of different cell types, such as primary dermal fibroblasts (hDF), SH-SY5Y neuroblastomas, and C2C12 myoblasts. High cell density and anisotropic growth were observed using fluorescence confocal microscopy on LCE scaffolds, with a four-fold increase in cell proliferation when compared with standard porous films. The study showed that the liquid crystal moieties' mobility and alignment within the LCEs greatly affect cell behavior, promoting aligned cell proliferation and improving tissue engineering results [84].

LCEs' work by Shaha et al. in both polydomain and monodomain configurations showed that the mesogen alignment and loading direction had a substantial impact on mechanical properties including stiffness, elasticity, and damping capacity. In contrast to polydomain LCEs, which showed more isotropic qualities, mechanical property testing revealed that monodomain LCEs showed increased stiffness and elasticity along the aligned mesogen direction. Monodomain LCEs have a strong anisotropic behavior, which is useful for applications that need directional mechanical features. This makes them particularly effective at simulating the complex mechanical environment found in the intervertebral disc. The in vivo investigations comprised subcutaneous implantation of both solid and porous LCEs in rats to evaluate tissue response and integration. The rats were monitored over the 12 weeks, and the results showed that LCEs are biocompatible, facilitating tissue encapsulation and ingrowth without causing detrimental effects on the surrounding tissues. Additionally, in vitro tests indicated that LCEs exhibit minimal swelling and maintain their mechanical integrity under simulated physiological conditions [85].

Overall, better cell alignment, proliferation, and differentiation can be achieved by LCEs by tailoring their mechanical properties and surface functions to resemble physiological settings. These characteristics demonstrate how LCEs can further tissue engineering and regenerative medicine.

3.4. Organ-on-a-Chip Applications

The traditional petri dish 2D system is by now over 100 years old [86]. The fast growth and easy experimental setup provided by these 2D systems is undeniable. Nonetheless, there is nothing that looks or behaves like a 2D system in any biological environment, so the results obtained from these systems may not translate well to the human body behavior of the same cells. Complexity is needed if one wants to study biological systems. Three-dimensional scaffolds help with this problem: the cells can grow in every direction, communicating properly with their neighbor cells, a closer behavior to the human body. Some drawbacks of this system are the inherent dark environment inside the 3D model, as it is sometimes difficult to observe what is happening to the cells inside the 3D scaffold, as well as the aggregates formed in 3D, creating a gradient of nutrient access and waste buildup [87].

Microfluidic organ-on-chip is a technology designed to overcome these difficulties. The device is designed to culture cells in a constantly moving environment, enclosed in a millimetric/micrometric chamber. This technology has the capacity of simulating the natural environment where the cells grow without the necessity of building the entire living organ [88]. The complexity of the microfluidic chip can increase as the necessity of the researcher needs, ranging from devices with a simple inlet and outlet to introduce flow [89] to as complex as introducing electric field gradients and producing dielectrophoresis effects inside the chip [90].

The addition of LC molecules into the organ-on-chip system clearly increases its potential uses. It has been shown that biological creatures like bacteria can be channeled and manipulated to follow specific paths using LC substrates [91], which can be considered a 2D system. Several studies dedicated to exploring the parameters of microfluidic channels as well as the anchoring condition of the LC molecule have concluded that by appropriately tuning these physical variables inside the chip, one can experimentally control and manipulate the profiles of flow velocity and director orientation across the channel [92]. It is still an open question whether biological entities like cells can be manipulated and sorted in these 3D microfluidic LC channels; nonetheless, the results and the direction of the latest experiments point out that those systems are close to being implemented.

4. Biosensing Applications

The use of liquid crystal-based biosensors has grown in recent years as a simple, direct, inexpensive, highly selective, and sensitive detection alternative. While there are only a few examples of LCEs as biosensors, we believe that it is important to mention early LC biosensors to encompass how these applications can potentially be the base for future LCE biosensor techniques. Gupta et al. described the construction of a cell composed of a gold thin film and a self-assembled monolayer in which target proteins, by binding to the surface of the monolayer, altered the roughness of the gold and consequently the orientation of the 4-cyano-4-pentylbiphenyl (5CB), allowing the amplification and transduction of signals in optical outputs [93]. Later, the group described the development of a system in which *"liquid crystals are used to amplify interfacial phenomena at fluid interfaces into optical images"* [94], inspired by earlier biomolecular investigations. 5CB is a widely used nematic liquid crystal whose orientational changes can easily be detected by polarized optical microscopy (POM). The apparatus consisted of treated glass surfaces as supports, copper grids to stabilize the nematic films (5CB), and an aqueous solution containing sodium dodecyl sulfate (SDS). The presence of SDS allows a reversible change from planar orientation (5CB-water interface) to homeotropic in the liquid crystalline bulk (Figure 8), which can be visualized under a polarized optical microscope (POM) [94]. This technique has opened the door to several other research projects that have revolutionized the field of biosensor technology.
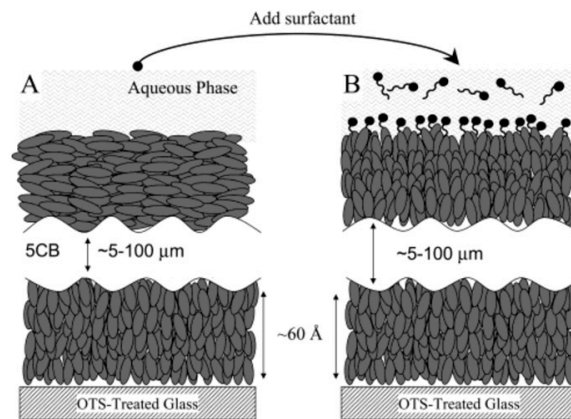
Figure 8. Representation of the 5CB-water interface: (**A**) in the absence of surfactant, 5CB has a planar orientation; (**B**) with the addition of surfactant, 5CB assumes a homeotropic configuration. Reprinted with permission from Brake and Abbott [92]. Copyright (2002) American Chemical Society.

With the aim of developing a simple and label-free tool for the diagnosis of pathogens such as bacteria and fungi, Khan et al. proposed the construction of a TEM grid cell composed of a nematic liquid crystal blend (E7), a cationic surfactant (DTAB), and a single-stranded DNA probe (ssDNA). E7 is a eutectic LC mixture made of four cyano-substituted polyphenyls prepared at a determined composition. E7 shows a single nematic to isotropic (NI) transition at around $T_{NI} = 61$ °C [95,96]. This mixture presents a wide range of operating temperatures and has been widely used in the preparation of polymer dispersed liquid crystal (PDLC) for applications in several types of display devices. The device proposed by Kahn, then, in the presence of the target DNA, induces a change in the orientation of the E7 molecules from homeotropic to planar (Figure 9), characterized by the transition from black to bright colors due to the birefringence of the planar phase observed under POM. This device allows the detection of *Rhazictonia solani* and *Erwinia carotovora* at concentrations ≥ 0.05 nM due to the signal amplification provided by the liquid crystal molecules, as well as allowing the differentiation of even 2–3 bp mismatches with the formation of different domains, guaranteeing high selectivity [97].
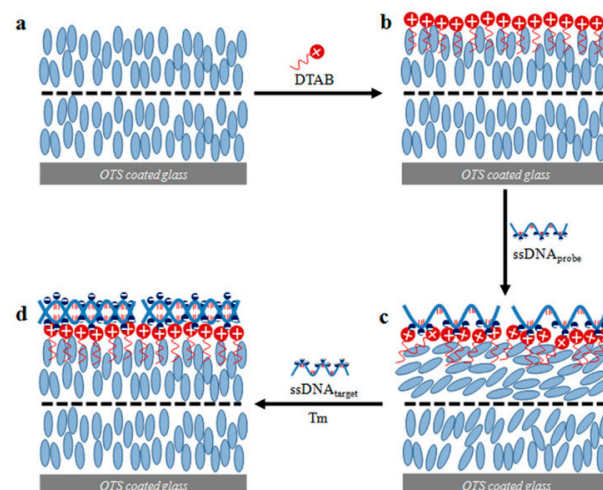
Figure 9. Illustration of the proposed LC cell for the detection of single-stranded DNA from *Rhazictonia solani* and *Erwinia carotovora*: (**a**) OTS-coated glass supporting TEM grid containing E7 molecules; (**b**) addition of surfactant (DTAB); (**c**) addition of single-stranded DNA probe causes orientation change to planar orientation; (**d**) addition and hybridization of DNA target causes homeotropic orientation. Reprinted from *Sci Rep* [95]. Copyright © (2016) with permission from Springer Nature.

In the race for diagnostic methods in the COVID-19 pandemic, liquid crystal-based biosensors emerged as a possible alternative. Researchers from The Ohio State University and Purdue University proposed using technology previously described in the literature to detect SARS-CoV-2 RNA from concentrations on the femtomolar (fM) scale; they developed a kit and smartphone app (Figure 10) that uses machine learning to classify image patterns and can provide a diagnosis quickly, easily, and affordably [98]. Figure 9 shows the LC device developed for the detection of SARS-CoV-2 RNA; in positive cases, the single-stranded RNA target hybridizes with the probe and promotes a change in orientation of E7 from planar to homeotropic in the aqueous interface, resulting in the disappearance of the birefringence and the formation of a dark pattern as observed on POM. The additional inset figures show the components of the device and the smartphone application developed for COVID diagnosis.
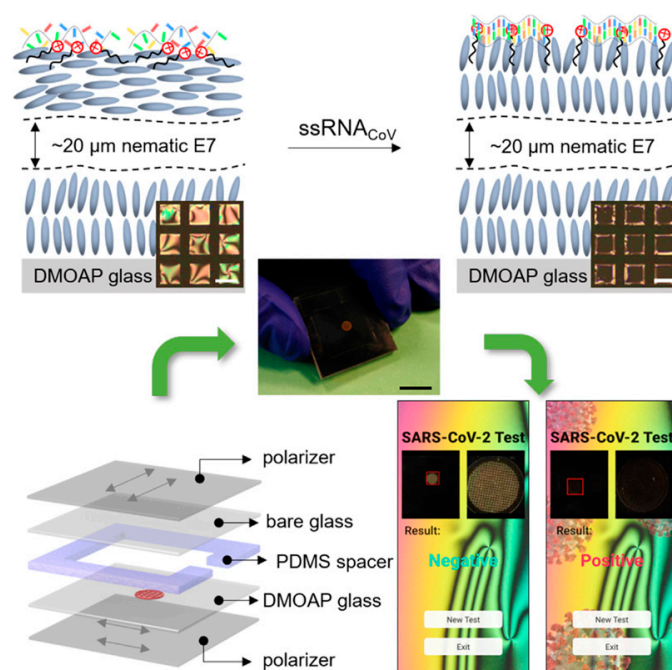

Figure 10. Liquid crystal cell developed for the detection of SARS-CoV-2 RNA; in positive cases, the single-stranded RNA target hybridizes with the probe and promotes a change in orientation, resulting in the formation of a dark pattern. Components of the device and smartphone application developed for COVID diagnosis. Reprinted from *Cell Rep Phys Sci* [96]. Copyright (2020) with permission from Elsevier.

The application of LC biosensors goes beyond what we can envision; they can become a new strategy for better detecting longtime known diseases. Insulin, for example, is one of the hormones that control the level of glucose in the blood [99] and is directly related to obesity, diabetes [100], and other illnesses. Liu et al. developed a sensor capable of measuring insulin between 0.1 and 10 nM within 5 min in diluted serum and urine samples. The apparatus consisted of a substrate containing a copper grid, immobilized dimethyloctadecyl[3-(trimethoxysilyl)propyl] ammonium chloride (DMOAP), and 5CB (Figure 11A), which has a homeotropic orientation in the presence of cetyltrimethylammonium bromide (CTAB) (Figure 11B). The G-quadruplex aptamer (IGA3) interacts electrostatically with the surfactant CTAB (Figure 11C), and upon binding to the insulin in the sample, IGA3 undergoes a conformational change to stretch, which consequently induces a planar orientation in the liquid crystal (Figure 11D) [101]. Figure 10 shows that when 5CB is in the homeotropic orientation (B–C), a dark image is formed, while in the presence of insulin, there is a change in orientation and the image obtained is bright.
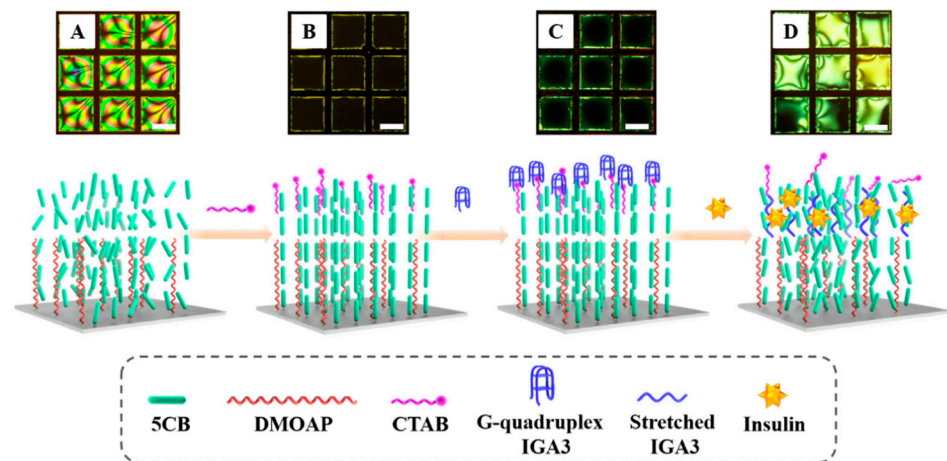
Figure 11. Optical patterns observed in POM: (**A**) Cell containing a glass substrate, copper grid, immobilized DMOAP, and 5CB in PBS medium; (**B**) homeotropic orientation in the presence of CTAB; (**C**) IGA3 interacts electrostatically with CTAB; (**D**) in the presence of insulin, IGA3 is stretched and induces a planar orientation in 5CB. Reprinted from *J Colloid Interf Sci* [99]. Copyright (2022) with permission from Elsevier.

Parkinson's disease is one of the most common disorders affecting the elderly in North America and other parts of the world [102]. Previous studies by Zheng et al. identified DNA aptamers (F5R1 and F5R2) that efficiently bind to one of the potential Parkinson's disease biomarkers, the alpha-synuclein protein [103]. Based on these studies, Yang et al. proposed the use of the F5R1 structure to obtain a simple and inexpensive method for early diagnosis. The device consists of a gold-coated glass and a self-assembled monolayer (C10SH + C16SH) with the aptamer immobilized on the underside of the substrate. The cell is filled with 5CB and has a homeotropic orientation in the absence of a biomarker, which is disrupted by the folding of the DNA when it binds to the target protein, resulting in a change from dark to bright under the POM due to the planar alignment of the LC (Figure 12A). Tests showed a detection range of 50–400 nM and a low level of non-specific interactions with the controls used, despite lower sensitivity than ELISA tests [104]. Subsequently, they proposed another alternative to overcome some of the limitations found in the previously described method, such as the cost and preparation of the substrate, detection time, and sensitivity. This time, they used the gold grid on a DMOAP-coated substrate and CTAB at the LC-aqueous interface, with the same F5R1 aptamer used in the previous studies, resulting in a detection limit for alpha-synuclein of 10 pM (Figure 12B) [105].
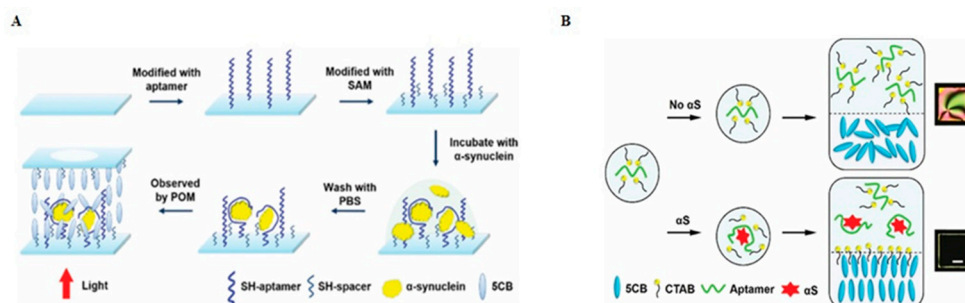
Figure 12. (**A**) Proposed model with a detection range of 50–400 nM of alpha-synuclein. Adapted with permission of [100] Copyright (2020) permission conveyed through Copyright Clearance Center, Inc., (**B**) Optimizations performed on the biosensor resulted in a detection limit for alpha-synuclein of 10 pM. Adapted with permission from Yang et al. [103], permission conveyed through Copyright Clearance Center, Inc.

Alzheimer's disease (AD) is another prevalent disease affecting the elderly. It was estimated that 6.7 million Americans over the age of 65 would be affected by AD in 2023, a number that is expected to nearly double by the year 2060 [106,107]. Thus, there is a desperate need for new tools for early diagnosis that are fast, cost-effective, and sensitive. In the search for new sensors, Kemiklioglu et al. developed a device that uses amyloid-beta-42 (Ab42) immunocomplex formation events as a strategy for detecting and diagnosing AD. The device consists of a glass coated with DMOAP filled with LCs (5CB) in which antibodies against Ab42 have been immobilized (Figure 13A–D). As a result, the addition of the Ab42 peptide was able to promote a change in the orientation of the LCs due to the formation of the antibody-antigen binding (Figure 13E); even at antigen concentrations as low as 1 pg/mL, Apolipoprotein E4 (ApoE4) was also added to evaluate the possible effects of its binding to the antigen in the presence of 5CB (Figure 13F); unfortunately, the effects observed were less pronounced than those of the antibody-antigen complex [108].
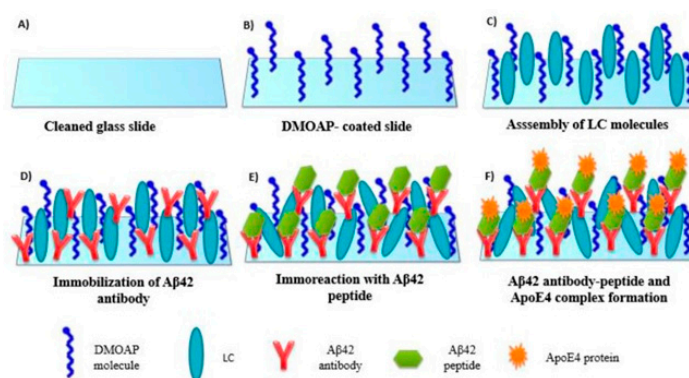

Figure 13. (**A**) Cleaned glass is used as a substrate; (**B**) DMOAP is used to coat the substrate; (**C**) the cell is filled with 5CB; (**D**) immobilization of antibody; (**E**) antibody-antigen binding process; (**F**) ApoE4 addition and complex formation. Reprinted from *J Biosci Bioeng* [106]. Copyright (2021) with permission from Elsevier.

Another example is acetylcholine (ACh), known as a neurotransmitter that is maintained at regulated levels for the transmission of nerve signals in a healthy organism. The enzyme acetylcholinesterase (AChE) is responsible for converting ACh to choline and acetic acid; however, due to certain factors, such as the pesticides malathion and fenobucarb, this activity is inhibited and can lead to continuous stimulation, which can cause fatal effects [109]. Inspired by the work of Wang et al. on the development of liquid crystal platforms for the evaluation of AChE [110,111] and enzymatic activity studies in microcapillaries [112,113], Nguyen et al. used OTS-coated microcapillaries containing 5CB droplets that form a monolayer in the presence of surfactant myristoylcholine chloride (Myr) and a four-petal pattern (Figure 14A–C). Once the enzyme AChE is present in the medium, it promotes the conversion of Myr to myristic acid and choline, preventing the formation of the monolayer and resulting in a bright double line pattern (Figure 14D). In the presence of malathion and fenobucarb, the enzymatic action is inhibited, and the double line pattern is not observed [114].

LCs can also be used as sensors to detect environmental pollutants that directly affect human health. It is known that mercury ions are highly toxic to living organisms and are unfortunately widely found as contaminants in water sources. One strategy for monitoring the contamination levels of this heavy metal uses octadecyltrichlorosilane (OTS)-coated glass with a TEM grid on top and a mixture of 5CB and potassium N-methyl-N-dodecyldithiocarbamate (MeDTC). MeDTC is used as a specific chelating agent for Hg^{2+} ions, which acts at the aqueous interface and promotes a change in the orientation of 5CB when the complex with mercury ions is formed (Figure 15). The detection limit of the described technique is 0.5 mM, and other common interferents present in the samples analyzed did not promote responses [115].
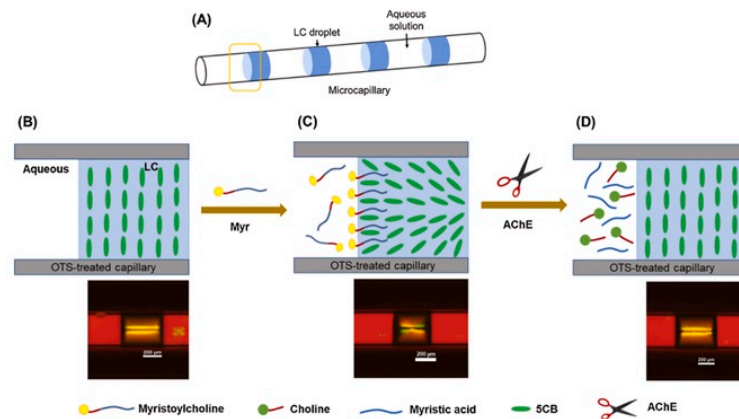
Figure 14. (**A**) OTS-coated microcapillaries containing 5CB droplets; (**B**) sensor in PBS medium; (**C**) Myr addition; (**D**) enzymatic cleavage of Myr to myristic acid and choline. The bottom shows the images corresponding to each POM event. Reprinted from *Colloids Surf B Biointerfaces* [112]. Copyright (2021) with permission from Elsevier.
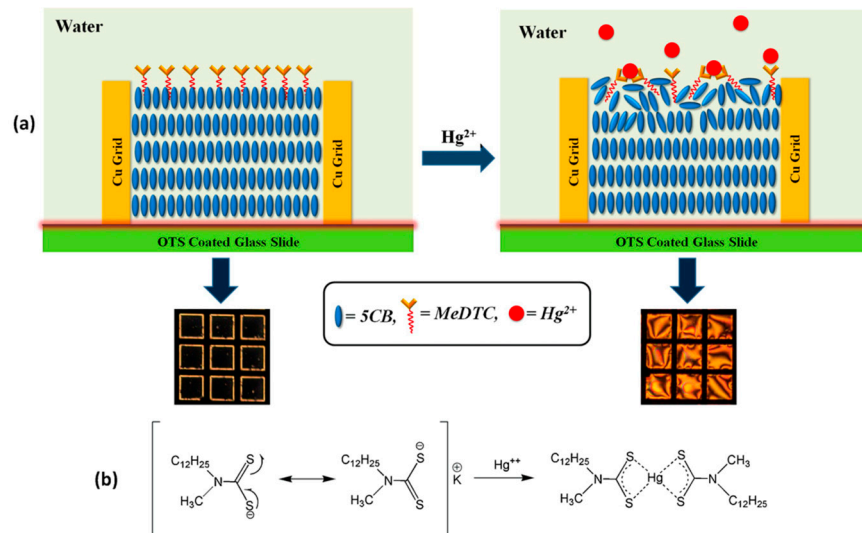
Figure 15. (**a**) Change in the 5CB orientation due to complexation MeDTC-Hg^{2+}, (**b**) Chemistry of MeDTC-Hg^{2+} complexation. Reprinted from *Sensor Actuat B-Chem* [113] Copyright (2016) with permission from Elsevier.

Firefighters and first responders are the most exposed to adverse environmental situations where toxic gases such as chlorine (Cl_2) or phosgene ($COCl_2$) are often present. Protective equipment helps reduce the effects of these exposures, but they are still at risk when these protective measures are removed before they can predict if all toxic gases resulting during a fire have been eliminated. In most cases, one of the team members is responsible for measuring the gases with a portable device, but often this measure is not effective in reflecting the reality of each team member's exposure. Based on this shortcoming, Prévôt et al. presented a zero-power sensor capable of measuring acute and chronic exposure at ppm levels. Nanoparticles containing reactive ligands are used as ink to print warning signs on a glass substrate. The cell is filled with nematic LCs that have a homeotropic orientation in the absence of hazardous chemicals. When exposed to gases such as Cl_2, the transition to planar anchoring takes place and forms the unmistakable warning signal that can be observed under crossed polarizers (Figure 16) [116].
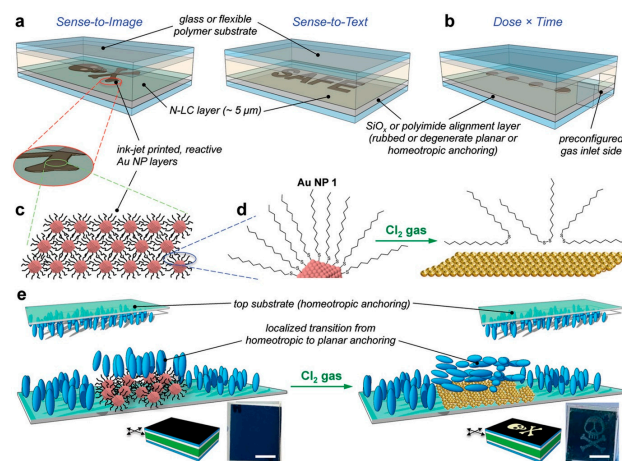
Figure 16. (**a**) Schematic representation of sensor models (figure and text); (**b**) representation of the sensor based on dose x exposure time; (**c**) Au NP pattern created by ink jet printer; (**d**) chemical reaction between Au NP and Cl_2; (**e**) change in orientation of N-LC in the presence of Cl_2. Reprinted from *Adv Mater Technol-Us* [114]. Copyright (2020) with permission from John Wiley and Sons.

Liquid crystals can also be combined with polymeric materials to create advanced sensors. Ailincai et al. prepared droplets (2–5 mm) using a microemulsion technique with different mass fractions between a cholesteric LC, cholesterol acetate (*L*-ChAc), and a polymeric matrix composed of polyvinyl alcohol boric acid (PVAB). The LC in the matrix exhibits planar anchoring, and changes in orientation were observed by different optical textures in the presence of sugars (*D*-glucose, *D*-galactose), amino acids (*D*-alanine, *L*-arginine), and DNA (salmon sperm), making the material promising in the field of biosensing [117]. The combination of LC and block copolymers for protein detection is another example found in the literature [118]. A TEM grid cell consisting of an interface between water and 5CB modified by the presence of PAA-b-LCP block copolymer (where PAA refers to poly(acrylic acid) and LCP to poly(4-cyanobiphenyl-4-oxy-undecylacrylate) was used as a method for the detection of albuminuria in urine samples, described by Khan et al. [119]. More recently, devices based on cholesteric LCE exhibit different colors when exposed to different mechanical stimuli, such as stretching or compression [120], under linear polarization and can be used as strain sensors or even in soft robots [121].

The use of LCEs in biological and medical applications will no doubt continue to increase as researchers develop more novel elastomers. Use of LC devices as sensors has been widely shown to be a successful application, and this function could easily translate into the medical setting in the form of diagnostic tools [122]. The intrinsic characteristics of LCEs, such as responsiveness to heat, light, and mechanical stress, may be harnessed in the development of diagnostic tools and imaging techniques. For example, various health conditions are associated with temperature variations in the body or in body parts, including cancer [123], blood clots [124], and infections [125].

For example, Li et al. designed LCE microspheres (LCEM) for use as pH sensors (Figure 17). Horseradish peroxidase (HRP) was immobilized on the microspheres (LCEM-HRP), which adopted two different configurations—radial and concentric. The configuration of the LCEM-HRP was dependent on the pH of the medium, and they were tested with various cells and found to be compatible. In addition, this detection method displayed single-cell resolution. The ability to determine the pH of individual cells could be applicable in the detection of cancer, since the pH of healthy cells is neutral while cancer cells exhibit a slightly acidic pH. These promising results indicate that novel LCE materials can be designed to aid in the diagnosis of medical conditions [126].
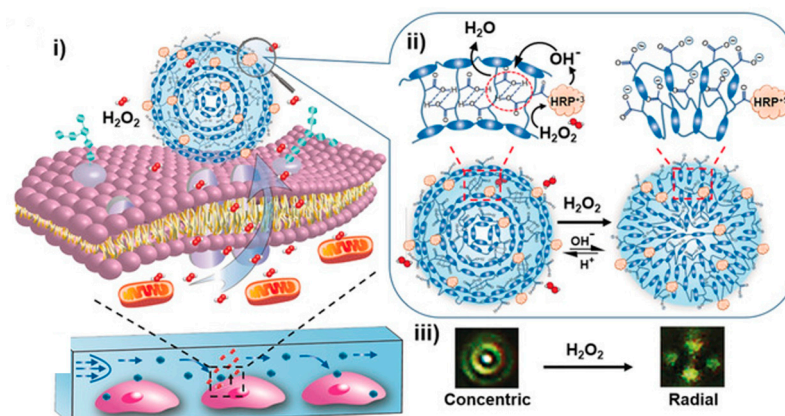
Figure 17. (**i**) Liquid crystal elastomer microspheres functionalized with horseradish peroxidase (LCEM-HRP) immobilized on the cell membrane; (**ii**) the concentric and radial configurations of the LCEM-HRP, which transform in the presence of H_2O_2; and (**iii**) POM (polarized optical microscope) images of the LCEM-HRP in the two configurations. Reprinted from *Angewandte Chemie* [124] Copyright (2020) with permission from Wiley.

Abadia et al. investigated biocatalytic LCE sensors for urea detection. In this case, urease is immobilized on the film, and the enzymatic response is transduced on a large scale due to the decrease in liquid crystalline order caused by the formation of ammonia [78]. Another use of LCE is in the detection of organophosphates such as malathion. In this case, Abadia et al. proposed a film made of *N,N*-dimethylethylenediamine (DMEN) and 1,4-bis-[4-(6acryloyloxyhexyloxy)benzoyloxy-2-methylbenzene (C6M). The LCE in this work was used to detect toxic pesticides by immobilizing hydrolytic pig liver esterase (PLE). In the presence of malathion, the PLE enzyme promotes catalytic hydrolysis to form malathion monoacid, which in turn changes the pH of the medium and induces a conformational change from a ribbon-like to a helical shape (see Figure 18). The sensor provides a quantitative relationship between the helical pitch change and a specific exposure dose and is not affected by environmental variations and other chemical interferences [127].
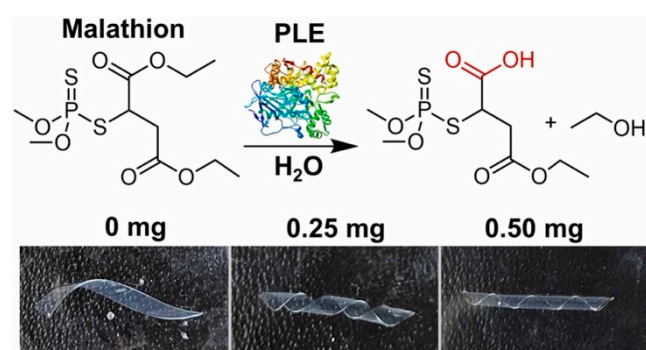
Figure 18. Malathion sensing using PLE-containing LCEs, showing the schematic of PLE hydrolysis of malathion into malathion monoacid. Malathion monoacid lowers the pH of the solution, triggering a response in the LCE. LCE ribbons in the presence of several doses of malathion at room temperature show the formation of a helix and the impact of the malathion dose on the helical pitch. Reprinted from *Sensors and Actuators B: Chemical* [125]. Copyright (2024) with permission from Elsevier.

## 5. 3D and 4D Printing of LCEs

5.1. 3D Printing

Digital Light Processing (DLP) stereolithography is effectively used for 3D printing LCEs. This technique employs a photocurable resin cured layer-by-layer to create intricate 3D structures, incorporating LC moieties that promote cell alignment due to their

anisotropic ordering. A work by Prévôt et al. highlighted the successful use of a photocrosslinkable smectic-A (Sm-A) LCE for 3D printing, demonstrating its ability to promote cell proliferation and anisotropy. The study involved creating a digital 3D model of a brain structure, reproduced using a DLP printer. Synchrotron Small-Angle X-ray Diffraction (SAXD) data showed strong alignment of LCE layers, directing cell growth along anisotropic axes, essential for replicating organized native tissues and improving in vitro models [34].

Other 3D printing techniques have also been utilized in the production of LCEs, including extrusion printing, which leads to director alignment along the print line [27], as well as the ability to easily incorporate multiple materials into the same 3D printed object. This capability was shown by Jennifer Lewis, who reported the production of 3D-printed shape-memory LCEs that were not only actuated by temperature changes but also underwent network reconfigurations triggered by UV exposure by means of exchangeable dynamic bonds [128]. By exposing the LCE to UV while actuated, the programmed shape was "locked in". Multi-material printing was required to achieve this in 3D bulk scale, which was enabled by extrusion 3D printing of alternating layers of LCEs with and without the dynamic bonds.

In another display of multi-material printing, the same group developed a method of 3D printing "innervated" LCEs (iLCEs)—filaments containing a liquid metal (LM) core surrounded by a main chain LCE (Figure 19). They reported the design of a core-shell extrusion nozzle used to produce the iLCEs, which were printed in the nematic phase and UV-cured. Inclusion of the LM core allowed for actuation of the iLCE via joule heating and cooling induced by power input through the filament. Upon heating, the filaments contracted in the printing direction and were shown to lift over 200 times the LCE weight while doing so. The team also demonstrated the ability to program a desired shape for the iLCE, which was maintained in a closed-loop feedback system driven by sensation of the resistance of the iLCE fiber [129].
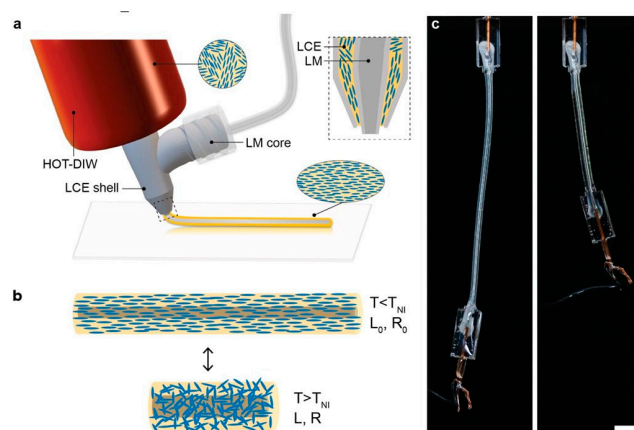
Figure 19. Innervated LM-LCE fibers. (**a**) Schematic illustration of core-shell 3D printing of iLCE fibers composed of a liquid metal (LM) core surrounded by a liquid crystal elastomer (LCE) shell, whose director is aligned along the print path. (**b**) Schematic illustration of iLCE actuation when cycled above and below the LCE nematic-to-isotropic transition temperature, TNI. (**c**) Images of an iLCE fiber before (**left**) and after (**right**) joule heating above TNI (scale bar = 5 mm). Reprinted from *Adv Mater* [127] Copyright (2021) with permission from Wiley.

5.2. 4D Printing

Significant progress has been achieved in 4D printing with LCEs pioneered by T. Ware using direct-write printing to create 3D structures capable of reversible shape changes by controlling the alignment of LC molecules during the printing process. With the use of this method, intricate, responsive structures capable of large deformations, alike volumetric contractions and snap-through transitions, could be fabricated and utilized in soft robotics

and medical devices [130]. Proceeding from this basis, their work concentrated on modifying these LCEs at the molecular level to improve their actuation properties. By employing a two-stage thiol-acrylate reaction, they were able to fine-tune the material's network architecture, allowing for precise, programmable shape changes in response to thermal stimuli. This work demonstrated the potential for highly responsive and customizable actuators in smart material applications [131]. Later on, Ware's team introduced a novel approach by combining liquid metal with LCEs, resulting in 4D-printed composites that not only exhibited shape-changing properties but also enhanced electrical conductivity. This breakthrough opened new possibilities for multifunctional materials in soft electronics [65]. That same year, they explored the use of photo switchable actuators by incorporating azobenzene-based liquid crystals, enabling light-controlled, reversible shape changes. This innovation further demonstrated the versatility of 4D printing for creating adaptive systems [132]. Consequently, the group pushed the boundaries of 4D printing by adding living materials into their processes. By embedding bacteria into LCEs, they developed structures that could interact with their environment, paving the way for responsive, living systems with potential applications in healthcare and environmental monitoring [130].

McDougall et al. proposed greater efficiency and simplicity by eliminating external supports through embedded printing, which promotes the extrusion of LCE (75/25 wt% RM82:RM257) inside an easily removable gelatinous matrix (composed of water and laponite). Essential mechanical properties are attained with trifunctional acrylate, and the structure is cured with UV light, allowing reversible 3D shape changes upon heating, which can be applied to biomedical and wearable devices [131]. The above examples highlight the profound impact of 4D printing technologies on various fields, showcasing the potential for creating advanced, multifunctional materials.

6. Challenges and Limitations

While LCEs show potential for various biological applications, one of the key limitations for utilizing LCEs in biological applications is biocompatibility. When these materials contact biological tissues, they must not cause toxicity or unfavorable immune responses [132]. To determine their safety, extensive in vitro and in vivo testing is necessary, which can be expensive and time-consuming [133].

Another significant limitation is the degradation and longevity of LCEs within biological environments. They must maintain their structural integrity and functional properties over extended periods for long-term applications, such as implants or biosensors. For their practical application, they must be resistant to the biochemical conditions of the human body, which include temperature, pH, and different biochemicals [134].

The contact between the material and biological tissues must be carefully considered when integrating LCEs with biological systems. It is crucial to minimize inflammatory reactions and adhere properly. The main challenge is creating an interface that focuses on biological interactions with the ordering transitions in the LC systems. Accurate manipulation of the mechanical attributes, like elasticity and strength, is also necessary to satisfy the various demands of various biomedical uses. Partially crosslinked elastomers have limited applicability in situations where precise mechanical behavior is essential, including artificial muscles and responsive implants, due to their difficulty in spatially altering the direction of deformation [135].

The production processes for LCEs are often complex and require specialized equipment, posing practical limitations on their widespread adoption. Producing these materials at the scale required for clinical usage might be difficult due to the complexity and high cost of their synthesis and manufacture. Another area that needs further work for sophisticated optical applications in biological contexts is controlling optical qualities similar to auxetic behavior and transparency under physiological conditions [132].

Some of these challenges have been addressed by recent developments. Processing methods include surface alignment, magnetic fields, mechanical straining, and 4D, which have printing and have made it possible to create LCEs with a variety of mechanical charac-

teristics and shape-changing behaviors. For instance, surface alignment techniques enable the creation of LCE films as substrates or coatings for flexible electronics, while 4D printing makes it possible to fabricate LCE actuators that can mimic the forces generated by human muscles. Furthermore, rheological research on biocompatible and biodegradable LCE inks has shed light on how to create and print new materials with desirable characteristics for specific uses [134].

7. Conclusions and Future Perspectives

7.1. Material Innovations

Recent advancements in the field of LCEs facilitate creative applications in a wide range of industries. The synthesis and orientation of LCEs have been one of the most key areas of development [28,42,43,52,63,135]. These developments have made it possible to produce materials that can fulfill the demanding specifications of applications in robotics, optics, and other areas [136].

Photothermal-driven LCEs are the result of researchers' efforts to improve the mechanical characteristics and responsiveness of LCEs to outside stimuli, such as heat and light. These materials have enormous potential for application in soft robotics, a field that depends heavily on controlled and exact movements. The photothermal effect in LCEs influences the ability of these materials to convert absorbed light into heat, leading to localized temperature changes. The LCEs undergo a phase transition because of this temperature difference, which modifies their molecular alignment and results in a reversible shape change. This effect's precision is important because it permits precisely controlled deformation that can be altered by varying the light's intensity, wavelength, and exposure time. For example, LCEs exposed to near-infrared (NIR) light can actuate quickly and significantly, which is important for applications that need a small amount of energy input and quick response times [136].

Another area of innovation is the integration of LCEs with other smart materials to create composites that exhibit enhanced functionalities. For example, combining LCEs with liquid metals made from 75% gallium and 25% indium results in soft, flexible composites that incorporate the beneficial aspects of both materials. Because of their exceptional mechanical strength and excellent conductivity, these composite materials are well suited for use in flexible electronics and wearable technology [137]. Furthermore, by adding magnetic nanoparticles to LCE matrices, magnetic composite films have been created, opening new possibilities, including remote actuation and enhanced magnetic field responsiveness [138].

Researchers introduced carbon fiber reinforcement to LCEs to improve their mechanical properties. Because of this integration, LCEs' tensile strength and endurance are significantly increased, making them appropriate for demanding applications in the aerospace and automotive industries. Due to their increased structural support and high strength-to-weight ratio, carbon fibers enhance the mechanical performance of LCE composites overall. For components that experience directional stress, such as airplane wings and automobile chassis, uniform load distribution is ensured by aligning carbon fibers within the LCE matrix. Moreover, carbon fibers' thermal conductivity aids in controlling the heat produced during LCE actuation, extending the operational lifespan of these composites [139].

A unique path of innovation in LCE applications was established by Mistry et al., who reported in 2018 the synthesis and characterization of acrylate-based LCEs with inherent auxeticity without porosity and suggested that these could be designed so as to tune the auxetic response [140]. This was later demonstrated in 2024 by Cooper et al. by the synthesis of the same acrylate nematic LCEs, whose optical and physical properties could be adjusted by their composition and synthetic conditions [141]. Auxetic materials present a negative Poisson's ratio: when the material is exposed to an applied extension along one axis, then the material will expand in the directions perpendicular to that axis. These unique materials are known to have impact resistance, shear resistance, and fracture toughness, among other desired properties [142]. The development of auxetic LCEs offers promising prospects for

their use in various biological applications, such as cardiac stents [143], contact and other optical lenses [141,144], and sports helmets [145].

7.2. Expanding Biological Applications

Liquid crystal elastomers (LCEs) are a remarkable new material with diverse applications in medicine and biology. Their exceptional adaptability and ability to respond to external stimuli make them ideal for a wide range of applications. LCEs enable precise, environment-responsive medication release systems in drug delivery. In soft robotics, LCEs mimic natural muscle movements, advancing medical devices. For tissue engineering, LCEs provide customizable scaffolds for improved cell growth. In biosensing, LCEs offer potential for advanced wearable and environmental sensors. LCEs' tunable properties, including shape memory and anisotropic responses, allow for creative designs in biomedical engineering, including for load-bearing biomedical applications. However, challenges remain in ensuring biocompatibility, maintaining long-term stability, and achieving cost-effective production. Future research should focus on improving mechanical characteristics, reinforcing integration with biological systems, and developing innovations like photothermal-driven LCEs and advanced composites. LCEs show great promise for revolutionizing biological applications. Ongoing research and development will be crucial to fully realizing their potential in advancing medical and technological fields.

References

1. Lehmann, O. Über fliessende krystalle. *Z. Phys. Chem.* **1889**, *4*, 462–472. [CrossRef]
2. Reinitzer, F. Beiträge zur Kenntnis des Cholesterins. *Monatshefte Chem.* **1888**, *9*, 20. [CrossRef]
3. Lehmann, O. Les cristaux liquides. *J. Phys. Theor. Appl.* **1909**, *8*, 713–735. [CrossRef]
4. de Gennes, P.G. A semi-fast artificial muscle. *Comptes Rendus L'Acad. Sci. Ser. IIB Mech. Phys. Chem. Astron.* **1997**, *5*, 343–348. [CrossRef]
5. de Gennes, P.G.; Hebert, M.; Kant, R. Artificial muscles based on nematic gels. *Macromol. Symp.* **1997**, *113*, 39–49. [CrossRef]
6. Warner, M.; Terentjev, E. *Liquid Crystal Elastomers*; Oxford University Press (OUP): Oxford, UK, 2003. [CrossRef]
7. Yakacki, C.M.; Saed, M.; Nair, D.P.; Gong, T.; Reed, S.M.; Bowman, C.N. Tailorable and programmable liquid-crystalline elastomers using a two-stage thiol-acrylate reaction. *RSC Adv.* **2015**, *5*, 18997–19001. [CrossRef]
8. Martella, D.; Paoli, P.; Pioner, J.M.; Sacconi, L.; Coppini, R.; Santini, L.; Lulli, M.; Cerbai, E.; Wiersma, D.S.; Poggesi, C.; et al. Liquid Crystalline Networks toward Regenerative Medicine and Tissue Repair. *Small* **2017**, *13*, 1702677. [CrossRef] [PubMed]
9. Ito, Y.; Chen, X.; Kang, I.-K. *Advances in Bioinspired and Biomedical Materials Volume 2*; ACS Symposium Series; American Chemical Society: Washington, DC, USA, 2017; Volume 1253.
10. Barón, M. Definitions of basic terms relating to low-molar-mass and polymer liquid crystals. *Pure Appl. Chem.* **2001**, *73*, 845–895. [CrossRef]
11. Kerkam, K.; Viney, C.; Kaplan, D.; Lombardi, S. Liquid crystallinity of natural silk secretions. *Nature* **1991**, *349*, 596–598. [CrossRef]
12. Willcox, P.J.; Gido, S.P.; Muller, W.; Kaplan, D.L. Evidence of a Cholesteric Liquid Crystalline Phase in Natural Silk Spinning Processes. *Macromolecules* **1996**, *29*, 5106–5110. [CrossRef]
13. Fontana, F.; Bellini, T.; Todisco, M. Liquid Crystal Ordering in DNA Double Helices with Backbone Discontinuities. *Macromolecules* **2022**, *55*, 5946–5953. [CrossRef]
14. Saw, T.B.; Doostmohammadi, A.; Nier, V.; Kocgozlu, L.; Thampi, S.; Toyama, Y.; Marcq, P.; Lim, C.T.; Yeomans, J.M.; Ladoux, B. Topological defects in epithelia govern cell death and extrusion. *Nature* **2017**, *544*, 212–216. [CrossRef] [PubMed]
15. Eggleson, K.K. Stem cell-based therapies: Promises, obstacles, discordance, and the agora. *Perspect. Biol. Med.* **2012**, *55*, 1–25. [CrossRef] [PubMed]
16. Prévôt, M.; Bergquist, L.; Sharma, A.; Mori, T.; Gao, Y.; Bera, T.; Zhu, C.; Leslie, M.; Cukelj, R.; Korley, L.T.J.; et al. *New Developments in 3D Liquid Crystal Elastomers Scaffolds for Tissue Engineering: From Physical Template to Responsive Substrate*; SPIE: Philadelphia, PA, USA, 2017.

17. Prévôt, M.E.; Ustunel, S.; Bergquist, L.E.; Cukelj, R.; Gao, Y.; Mori, T.; Pauline, L.; Clements, R.J.; Hegmann, E. Synthesis of Biocompatible Liquid Crystal Elastomer Foams as Cell Scaffolds for 3D Spatial Cell Cultures. *J. Vis. Exp.* **2017**, *122*, e55452. [CrossRef]

18. Ustunel, S.; Prévôt, M.E.; Rohaley, G.A.R.; Webb, C.R.; Yavitt, B.; Freychet, G.; Zhernenkov, M.; Pindak, R.; Schaible, E.; Zhu, C.; et al. Mechanically tunable elastomer and cellulose nanocrystal composites as scaffolds for in vitro cell studies. *Mater. Adv.* **2021**, *2*, 464–476. [CrossRef]

19. Prévôt, M.; Hegmann, E. From Biomaterial, Biomimetic, and Polymer to Biodegradable and Biocompatible Liquid Crystal Elastomer Cell Scaffolds. In *Advances in Bioinspired and Biomedical Materials Volume 2*; ACS Symposium Series; American Chemical Society: Washington, DC, USA, 2017; Volume 1253, pp. 3–45.

20. Cheng, H.; Hill, P.S.; Siegwart, D.J.; Vacanti, N.; Lytton-Jean, A.K.R.; Cho, S.W.; Ye, A.; Langer, R.; Anderson, D.G. A Novel Family of Biodegradable Poly(ester amide) Elastomers. *Adv. Mater.* **2011**, *23*, H95–H100. [CrossRef]

21. Novak, U.; Kaye, A.H. Extracellular matrix and the brain: Components and function. *J. Clin. Neurosci.* **2000**, *7*, 280–290. [CrossRef] [PubMed]

22. Bartolo, P.; Domingos, M.; Gloria, A.; Ciurana, J. BioCell Printing: Integrated automated assembly system for tissue engineering constructs. *CIRP Ann.* **2011**, *60*, 271–274. [CrossRef]

23. Guo, H.; Saed, M.O.; Terentjev, E.M. Thiol–acrylate side-chain liquid crystal elastomers. *Soft Matter* **2022**, *18*, 4803–4809. [CrossRef]

24. Ustunel, S.; Prévôt, M.E.; Clements, R.J.; Hegmann, E. Cradle-to-cradle: Designing biomaterials to fit as truly biomimetic cell scaffolds—A review. *Liq. Cryst. Today* **2020**, *29*, 40–52. [CrossRef]

25. Ustunel, S.; Sternbach, S.; Prévôt, M.E.; Freeman, E.J.; McDonough, J.A.; Clements, R.J.; Hegmann, E. 3D Co-culturing of human neuroblastoma and human oligodendrocytes, emulating native tissue using 3D porous biodegradable liquid crystal elastomers. *J. Appl. Polym. Sci.* **2023**, *140*, e53883. [CrossRef]

26. Gungor-Ozkerim, P.S.; Inci, I.; Zhang, Y.S.; Khademhosseini, A.; Dokmeci, M.R. Bioinks for 3D bioprinting: An overview. *Biomater. Sci.* **2018**, *6*, 915–946. [CrossRef] [PubMed]

27. Ambulo, C.P.; Burroughs, J.J.; Boothby, J.M.; Kim, H.; Shankar, M.R.; Ware, T.H. Four-dimensional Printing of Liquid Crystal Elastomers. *ACS Appl. Mater. Interfaces* **2017**, *9*, 37332–37339. [CrossRef] [PubMed]

28. Kotikian, A.; Truby, R.L.; Boley, J.W.; White, T.J.; Lewis, J.A. 3D Printing of Liquid Crystal Elastomeric Actuators with Spatially Programed Nematic Order. *Adv. Mater.* **2018**, *30*, 1706164. [CrossRef] [PubMed]

29. Mistry, D.; Traugutt, N.A.; Yu, K.; Yakacki, C.M. Processing and reprocessing liquid crystal elastomer actuators. *J. Appl. Phys.* **2021**, *129*, 130901. [CrossRef]

30. Prévôt, M.E.; Ustunel, S.; Yavitt, B.M.; Freychet, G.; Webb, C.R.; Zhernenkov, M.; Hegmann, E.; Pindak, R. Synchrotron Microbeam Diffraction Studies on the Alignment within 3D-Printed Smectic-A Liquid Crystal Elastomer Filaments during Extrusion. *Crystals* **2021**, *11*, 523. [CrossRef]

31. Sharma, A.; Neshat, A.; Mahnen, C.J.; Nielsen, A.D.; Snyder, J.; Stankovich, T.L.; Daum, B.G.; LaSpina, E.M.; Beltrano, G.; Gao, Y.; et al. Biocompatible, Biodegradable and Porous Liquid Crystal Elastomer Scaffolds for Spatial Cell Cultures. *Macromol. Biosci.* **2015**, *15*, 200–214. [CrossRef]

32. Sharma, A.; Mori, T.; Mahnen, C.J.; Everson, H.R.; Leslie, M.T.; Nielsen, A.d.; Lussier, L.; Zhu, C.; Malcuit, C.; Hegmann, T.; et al. Effects of Structural Variations on the Cellular Response and Mechanical Properties of Biocompatible, Biodegradable, and Porous Smectic Liquid Crystal Elastomers. *Macromol. Biosci.* **2017**, *17*, 1600278. [CrossRef]

33. Prévôt, M.E.; Andro, H.; Alexander, S.L.M.; Ustunel, S.; Zhu, C.; Nikolov, Z.; Rafferty, S.T.; Brannum, M.T.; Kinsel, B.; Korley, L.T.J.; et al. Liquid crystal elastomer foams with elastic properties specifically engineered as biodegradable brain tissue scaffolds. *Soft Matter* **2018**, *14*, 354–360. [CrossRef]

34. Prevot, M.E.; Ustunel, S.; Freychet, G.; Webb, C.R.; Zhernenkov, M.; Pindak, R.; Clements, R.J.; Hegmann, E. Physical Models from Physical Templates Using Biocompatible Liquid Crystal Elastomers as Morphologically Programmable Inks For 3D Printing. *Macromol. Biosci.* **2023**, *23*, e2200343. [CrossRef]

35. Ring, M.E. The history of maxillofacial prosthetics. *Plast. Reconstr. Surg.* **1991**, *87*, 174–184. [CrossRef]

36. Heng, W.; Solomon, S.; Gao, W. Flexible Electronics and Devices as Human–Machine Interfaces for Medical Robotics. *Adv. Mater.* **2022**, *34*, 2107902. [CrossRef]

37. Cianchetti, M.; Laschi, C.; Menciassi, A.; Dario, P. Biomedical applications of soft robotics. *Nat. Rev. Mater.* **2018**, *3*, 143–153. [CrossRef]

38. Cianchetti, M.; Laschi, C. Pleasant to the Touch: By Emulating Nature, Scientists Hope to Find Innovative New Uses for Soft Robotics in Health-Care Technology. *IEEE Pulse* **2016**, *7*, 34–37. [CrossRef] [PubMed]

39. Yin, R.; Wang, D.; Zhao, S.; Lou, Z.; Shen, G. Wearable Sensors-Enabled Human–Machine Interaction Systems: From Design to Application. *Adv. Funct. Mater.* **2021**, *31*, 2008936. [CrossRef]

40. Yu, H.; Gold, J.I.; Wolter, T.J.; Bao, N.; Smith, E.; Zhang, H.A.; Twieg, R.J.; Mavrikakis, M.; Abbott, N.L. Actuating Liquid Crystals Rapidly and Reversibly by Using Chemical Catalysis. *Adv. Mater.* **2024**, *36*, 2309605. [CrossRef]

41. McEvoy, M.A.; Correll, N. Materials that couple sensing, actuation, computation, and communication. *Science* **2015**, *347*, 1261689. [CrossRef]

42. Hua, Q.; Sun, J.; Liu, H.; Bao, R.; Yu, R.; Zhai, J.; Pan, C.; Wang, Z.L. Skin-inspired highly stretchable and conformable matrix networks for multifunctional sensing. *Nat. Commun.* **2018**, *9*, 244. [CrossRef] [PubMed]

43. Schwartz, M.; Lagerwall, J.P.F. Embedding intelligence in materials for responsive built environment: A topical review on Liquid Crystal Elastomer actuators and sensors. *Build. Environ.* **2022**, *226*, 109714. [CrossRef]

44. Hussain, M.; Jull, E.I.L.; Mandle, R.J.; Raistrick, T.; Hine, P.J.; Gleeson, H.F. Liquid Crystal Elastomers for Biological Applications. *Nanomaterials* **2021**, *11*, 813. [CrossRef]

45. Herbert, K.M.; Fowler, H.E.; McCracken, J.M.; Schlafmann, K.R.; Koch, J.A.; White, T.J. Synthesis and alignment of liquid crystalline elastomers. *Nat. Rev. Mater.* **2021**, *7*, 23–38. [CrossRef]

46. Resetic, A.; Milavec, J.; Bubnov, A.; Pociecha, D.; Hamplova, V.; Gorecka, E.; Zalar, B.; Domenici, V. New Liquid Crystalline Elastomeric Films Containing a Smectic Crosslinker: Chemical and Physical Properties. *Crystals* **2023**, *13*, 96. [CrossRef]

47. Wang, Y.; Liu, J.; Yang, S. Multi-functional liquid crystal elastomer composites. *Appl. Phys. Rev.* **2022**, *9*, 011301. [CrossRef]

48. Brannum, M.T.; Steele, A.M.; Venetos, M.C.; Korley, L.T.J.; Wnek, G.E.; White, T.J. Light Control with Liquid Crystalline Elastomers. *Adv. Opt. Mater.* **2019**, *7*, 1801683. [CrossRef]

49. Modes, C.; Warner, M. Shape-programmable materials. *Phys. Today* **2016**, *69*, 32–38. [CrossRef]

50. Babakhanova, G.; Turiv, T.; Guo, Y.; Hendrikx, M.; Wei, Q.H.; Schenning, A.; Broer, D.J.; Lavrentovich, O.D. Liquid crystal elastomer coatings with programmed response of surface profile. *Nat. Commun.* **2018**, *9*, 456. [CrossRef]

51. Pei, Z.; Yang, Y.; Chen, Q.; Terentjev, E.M.; Wei, Y.; Ji, Y. Mouldable liquid-crystalline elastomer actuators with exchangeable covalent bonds. *Nat. Mater.* **2014**, *13*, 36–41. [CrossRef]

52. Ware, T.H.; Perry, Z.P.; Middleton, C.M.; Iacono, S.T.; White, T.J. Programmable Liquid Crystal Elastomers Prepared by Thiol-Ene Photopolymerization. *ACS Macro Lett.* **2015**, *4*, 942–946. [CrossRef]

53. Godman, N.P.; Kowalski, B.A.; Auguste, A.D.; Koerner, H.; White, T.J. Synthesis of Elastomeric Liquid Crystalline Polymer Networks via Chain Transfer. *ACS Macro Lett.* **2017**, *6*, 1290–1295. [CrossRef]

54. Fowler, H.E.; Pearl, H.M.; Hoang, J.D.; White, T.J. Liquid Crystal Elastomers Prepared by Thiol-Ene Photopolymerization Amenable to Surface-Enforced Alignment. *Macromolecules* **2024**, *57*, 2619–2627. [CrossRef]

55. Prausnitz, M.R.; Mitragotri, S.; Langer, R. Current status and future potential of transdermal drug delivery. *Nat. Rev. Drug Discov.* **2004**, *3*, 115–124. [CrossRef] [PubMed]

56. Nozawa, I.; Suzuki, Y.; Sato, S.; Sugibayashi, K.; Morimoto, Y. Preparation of thermo-responsive membranes. II. *J. Biomed. Mater. Res.* **1991**, *25*, 577–588. [CrossRef]

57. Chen, K.; Lin, Y.; Lin, S. Thermally on-off switching nylon membrane for controlling drug penetration. *Drug Deliv. Syst.* **1996**, *11*, 55–61. [CrossRef]

58. Inoue, Y.; Atsumi, Y.; Kawamura, A.; Miyata, T. Thermoresponsive liquid crystalline polymer membranes that undergo phase transition at body temperature. *J. Membr. Sci.* **2019**, *588*, 117213. [CrossRef]

59. Stepulane, A.; Ahlgren, K.; Rodriguez-Palomo, A.; Rajasekharan, A.K.; Andersson, M. Lyotropic liquid crystal elastomers for drug delivery. *Colloid. Surface B* **2023**, *226*, 113304. [CrossRef]

60. Küpfer, J.; Finkelmann, H. Nematic liquid single crystal elastomers. *Die Makromol. Chem. Rapid Commun.* **1991**, *12*, 717–726. [CrossRef]

61. Brochu, P.; Pei, Q. Advances in dielectric elastomers for actuators and artificial muscles. *Macromol. Rapid Commun.* **2010**, *31*, 10–36. [CrossRef] [PubMed]

62. Kim, H.; Lee, J.A.; Ambulo, C.P.; Lee, H.B.; Kim, S.H.; Naik, V.V.; Haines, C.S.; Aliev, A.E.; Ovalle-Robles, R.; Baughman, R.H.; et al. Intelligently Actuating Liquid Crystal Elastomer-Carbon Nanotube Composites. *Adv. Funct. Mater.* **2019**, *29*, 1905063. [CrossRef]

63. Ambulo, C.P.; Ford, M.J.; Searles, K.; Majidi, C.; Ware, T.H. 4D-Printable Liquid Metal-Liquid Crystal Elastomer Composites. *ACS Appl. Mater. Interfaces* **2021**, *13*, 12805–12813. [CrossRef]

64. Xiao, Y.Y.; Jiang, Z.C.; Tong, X.; Zhao, Y. Biomimetic Locomotion of Electrically Powered "Janus" Soft Robots Using a Liquid Crystal Polymer. *Adv. Mater.* **2019**, *31*, e1903452. [CrossRef] [PubMed]

65. Shimoga, G.; Choi, D.-S.; Kim, S.-Y. Bio-Inspired Soft Robotics: Tunable Photo-Actuation Behavior of Azo Chromophore Containing Liquid Crystalline Elastomers. *Appl. Sci.* **2021**, *11*, 1233. [CrossRef]

66. Lu, X.; Zhang, H.; Fei, G.; Yu, B.; Tong, X.; Xia, H.; Zhao, Y. Liquid-Crystalline Dynamic Networks Doped with Gold Nanorods Showing Enhanced Photocontrol of Actuation. *Adv. Mater.* **2018**, *30*, e1706597. [CrossRef]

67. Cheng, Y.C.; Lu, H.C.; Lee, X.; Zeng, H.; Priimagi, A. Kirigami-Based Light-Induced Shape-Morphing and Locomotion. *Adv. Mater.* **2020**, *32*, e1906233. [CrossRef]

68. Ma, S.; Li, X.; Huang, S.; Hu, J.; Yu, H. A Light-Activated Polymer Composite Enables On-Demand Photocontrolled Motion: Transportation at the Liquid/Air Interface. *Angew. Chem. Int. Ed. Engl.* **2019**, *58*, 2655–2659. [CrossRef]

69. Li, Y.; Teixeira, Y.; Parlato, G.; Grace, J.; Wang, F.; Huey, B.D.; Wang, X. Three-dimensional thermochromic liquid crystal elastomer structures with reversible shape-morphing and color-changing capabilities for soft robotics. *Soft Matter* **2022**, *18*, 6857–6867. [CrossRef]

70. Zhan, Y.; Broer, D.J.; Liu, D. Perspiring Soft Robotics Skin Constituted by Dynamic Polarity-Switching Porous Liquid Crystal Membrane. *Adv. Mater.* **2023**, *35*, e2211143. [CrossRef]

71. *Biomaterials Science: An Introduction to Materials in Medicine*; Elsevier: Amsterdam, The Netherlands, 2020.

72. Martino, F.; Perestrelo, A.R.; Vinarsky, V.; Pagliari, S.; Forte, G. Cellular Mechanotransduction: From Tension to Function. *Front. Physiol.* **2018**, *9*, 824. [CrossRef]

73. Nguyen, A.T.; Sathe, S.R.; Yim, E.K. From nano to micro: Topographical scale and its impact on cell adhesion, morphology and contact guidance. *J. Phys. Condens. Matter* **2016**, *28*, 183001. [CrossRef]

74. Ye, K.; Wang, X.; Cao, L.; Li, S.; Li, Z.; Yu, L.; Ding, J. Matrix Stiffness and Nanoscale Spatial Organization of Cell-Adhesive Ligands Direct Stem Cell Fate. *Nano Lett.* **2015**, *15*, 4720–4729. [CrossRef]

75. Tse, J.R.; Engler, A.J. Stiffness gradients mimicking in vivo tissue variation regulate mesenchymal stem cell fate. *PLoS ONE* **2011**, *6*, e15978. [CrossRef]

76. Abadia, A.V.; Herbert, K.M.; White, T.J.; Schwartz, D.K.; Kaar, J.L. Biocatalytic 3D Actuation in Liquid Crystal Elastomers via Enzyme Patterning. *ACS Appl. Mater. Interfaces* **2022**, *14*, 26480–26488. [CrossRef]

77. Babakhanova, G.; Yu, H.; Chaganava, I.; Wei, Q.H.; Shiller, P.; Lavrentovich, O.D. Controlled Placement of Microparticles at the Water-Liquid Crystal Elastomer Interface. *ACS Appl. Mater. Interfaces* **2019**, *11*, 15007–15013. [CrossRef]

78. Babakhanova, G.; Krieger, J.; Li, B.X.; Turiv, T.; Kim, M.H.; Lavrentovich, O.D. Cell alignment by smectic liquid crystal elastomer coatings with nanogrooves. *J. Biomed. Mater. Res. A* **2020**, *108*, 1223–1230. [CrossRef]

79. Turiv, T.; Krieger, J.; Babakhanova, G.; Yu, H.; Shiyanovskii, S.V.; Wei, Q.H.; Kim, M.H.; Lavrentovich, O.D. Topology control of human fibroblast cells monolayer by liquid crystal elastomer. *Sci. Adv.* **2020**, *6*, eaaz6485. [CrossRef]

80. Agrawal, A.; Adetiba, O.; Kim, H.; Chen, H.; Jacot, J.G.; Verduzco, R. Stimuli-responsive liquid crystal elastomers for dynamic cell culture. *J. Mater. Res.* **2015**, *30*, 453–462. [CrossRef]

81. Herrera-Posada, S.; Mora-Navarro, C.; Ortiz-Bermudez, P.; Torres-Lugo, M.; McElhinny, K.M.; Evans, P.G.; Calcagno, B.O.; Acevedo, A. Magneto-responsive liquid crystalline elastomer nanocomposites as potential candidates for dynamic cell culture substrates. *Mater. Sci. Eng. C Mater. Biol. Appl.* **2016**, *65*, 369–378. [CrossRef]

82. Khoo, I.C.; Clements, R.J.; McDonough, J.A.; Freeman, E.J.; Korley, L.T.; Cukelj, R.; Leslie, M.T.; Zhu, C.; Bera, T.; Gao, Y.; et al. New developments in 3D liquid crystal elastomers scaffolds for tissue engineering: From physical template to responsive substrate. In Proceedings of the Liquid Crystals XXI, San Diego, CA, USA, 25 August 2017.

83. Shaha, R.K.; Merkel, D.R.; Anderson, M.P.; Devereaux, E.J.; Patel, R.R.; Torbati, A.H.; Willett, N.; Yakacki, C.M.; Frick, C.P. Biocompatible liquid-crystal elastomers mimic the intervertebral disc. *J. Mech. Behav. Biomed. Mater.* **2020**, *107*, 103757. [CrossRef]

84. Harrison, R.G. The outgrowth of the nerve fiber as a mode of protoplasmic movement. *J. Exp. Zool.* **2005**, *9*, 787–846. [CrossRef]

85. Duval, K.; Grover, H.; Han, L.H.; Mou, Y.; Pegoraro, A.F.; Fredberg, J.; Chen, Z. Modeling Physiological Events in 2D vs. 3D Cell Culture. *Physiology* **2017**, *32*, 266–277. [CrossRef]

86. Bhatia, S.N.; Ingber, D.E. Microfluidic organs-on-chips. *Nat. Biotechnol.* **2014**, *32*, 760–772. [CrossRef]

87. Gong, Y.; Fan, N.; Yang, X.; Peng, B.; Jiang, H. New advances in microfluidic flow cytometry. *Electrophoresis* **2018**, *40*, 1212–1229. [CrossRef]

88. Zhang, H.; Chang, H.; Neuzil, P. DEP-on-a-Chip: Dielectrophoresis Applied to Microfluidic Platforms. *Micromachines* **2019**, *10*, 423. [CrossRef]

89. Genkin, M.M.; Sokolov, A.; Lavrentovich, O.D.; Aranson, I.S. Topological Defects in a Living Nematic Ensnare Swimming Bacteria. *Phys. Rev. X* **2017**, *7*, 011029. [CrossRef]

90. Sengupta, A. Topological microfluidics: Present and prospects. *Liquid Cryst. Today* **2015**, *24*, 70–80. [CrossRef]

91. Gupta, V.K.; Skaife, J.J.; Dubrovsky, T.B.; Abbott, N.L. Optical Amplification of Ligand-ReceptorBinding Using Liquid Crystals. *Science* **1998**, *279*, 2077–2080. [CrossRef] [PubMed]

92. Brake, J.M.; Abbott, N.L. An experimental system for imaging the reversible adsorption of amphiphiles at aqueous-liquid crystal interfaces. *Langmuir* **2002**, *18*, 6101–6109. [CrossRef]

93. Bedjaoui, L.; Gogibus, N.; Ewen, B.; Pakula, T.; Coqueret, X.; Benmouna, M.; Maschke, U. Preferential solvation of the eutectic mixture of liquid crystals E7 in a polysiloxane. *Polymer* **2004**, *45*, 6555–6560. [CrossRef]

94. Nolan, P.; Tillin, M.; Coates, D. Liquid Crystal Microdroplet Composition in a UV Cured PDLC Film. *Mol. Cryst. Liq. Cryst. Lett.* **1992**, *8*, 129–135. [CrossRef]

95. Khan, M.; Khan, A.R.; Shin, J.H.; Park, S.Y. A liquid-crystal-based DNA biosensor for pathogen detection. *Sci. Rep.* **2016**, *6*, 22676. [CrossRef]

96. Xu, Y.; Rather, A.M.; Song, S.; Fang, J.C.; Dupont, R.L.; Kara, U.I.; Chang, Y.; Paulson, J.A.; Qin, R.; Bao, X.; et al. Ultrasensitive and Selective Detection of SARS-CoV-2 Using Thermotropic Liquid Crystals and Image-Based Machine Learning. *Cell Rep. Phys. Sci.* **2020**, *1*, 100276. [CrossRef] [PubMed]

97. Rahman, M.S.; Hossain, K.S.; Das, S.; Kundu, S.; Adegoke, E.O.; Rahman, M.A.; Hannan, M.A.; Uddin, M.J.; Pang, M.-G. Role of Insulin in Health and Disease: An Update. *Int. J. Mol. Sci.* **2021**, *22*, 6403. [CrossRef]

98. Olefsky, J.M. The insulin receptor: Its role in insulin resistance of obesity and diabetes. *Diabetes* **1976**, *25*, 1154–1162. [CrossRef] [PubMed]

99. Chen, J.M.; Liu, Z.P.; Yang, R.Z.; Liu, M.J.; Feng, H.Q.; Li, N.; Jin, M.L.; Zhang, M.M.; Shui, L.L. A liquid crystal-based biosensor for detection of insulin driven by conformational change of an aptamer at aqueous-liquid crystal interface. *J. Colloid. Interf. Sci.* **2022**, *628*, 215–222. [CrossRef] [PubMed]

100. Willis, A.W.; Roberts, E.; Beck, J.C.; Fiske, B.; Ross, W.; Savica, R.; Van Den Eeden, S.K.; Tanner, C.M.; Marras, C.; Parkinson's Foundation, P.G. Incidence of Parkinson disease in North America. *NPJ Park. Dis.* **2022**, *8*, 170. [CrossRef]

101. Zheng, Y.; Qu, J.; Xue, F.; Zheng, Y.; Yang, B.; Chang, Y.; Yang, H.; Zhang, J. Novel DNA Aptamers for Parkinson's Disease Treatment Inhibit α-Synuclein Aggregation and Facilitate its Degradation. *Mol. Ther.-Nucleic Acids* **2018**, *11*, 228–242. [CrossRef] [PubMed]
102. Yang, X.; Li, H.; Zhao, X.; Liao, W.; Zhang, C.X.; Yang, Z. A novel, label-free liquid crystal biosensor for Parkinson's disease related alpha-synuclein. *Chem. Commun.* **2020**, *56*, 5441–5444. [CrossRef]
103. Yang, X.; Zhao, X.; Liu, F.; Li, H.; Zhang, C.X.; Yang, Z. Simple, rapid and sensitive detection of Parkinson's disease related alpha-synuclein using a DNA aptamer assisted liquid crystal biosensor. *Soft Matter* **2021**, *17*, 4842–4847. [CrossRef]
104. *2023 Alzheimer's Disease Facts and Figures*, Wiley: Hoboken, NJ, USA, 2023. [CrossRef]
105. Rajan, K.B.; Weuve, J.; Barnes, L.L.; McAninch, E.A.; Wilson, R.S.; Evans, D.A. Population estimate of people with clinical Alzheimer's disease and mild cognitive impairment in the United States (2020–2060). *Alzheimers Dement.* **2021**, *17*, 1966–1975. [CrossRef] [PubMed]
106. Kemiklioglu, E.; Tuncgovde, E.B.; Ozsarlak-Sozer, G. Development of liquid crystal biosensor for the detection of amyloid beta-42 levels associated with Alzheimer's disease. *J. Biosci. Bioeng.* **2021**, *132*, 88–94. [CrossRef]
107. Mileson, B.E.; Chambers, J.E.; Chen, W.L.; Dettbarn, W.; Ehrich, M.; Eldefrawi, A.T.; Gaylor, D.W.; Hamernik, K.; Hodgson, E.; Karczmar, A.G.; et al. Common Mechanism of Toxicity: A Case Study of Organophosphorus Pesticides. *Toxicol. Sci.* **1998**, *41*, 8–20. [CrossRef]
108. Wang, Y.; Hu, Q.Z.; Guo, Y.X.; Yu, L. A cationic surfactant-decorated liquid crystal sensing platform for simple and sensitive detection of acetylcholinesterase and its inhibitor. *Biosens. Bioelectron.* **2015**, *72*, 25–30. [CrossRef] [PubMed]
109. Wang, Y.; Hu, Q.Z.; Tian, T.T.; Yu, L. Simple and sensitive detection of pesticides using the liquid crystal droplet patterns platform. *Sens. Actuat. B-Chem.* **2017**, *238*, 676–682. [CrossRef]
110. Kim, H.J.; Jang, C.H. Micro-capillary sensor for imaging trypsin activity using confined nematic liquid crystals. *J. Mol. Liq.* **2016**, *222*, 596–600. [CrossRef]
111. Rim, J.; Jang, C.H. Detection of catalase activity with aldehyde-doped liquid crystals confined in microcapillaries. *Anal. Biochem.* **2018**, *560*, 19–23. [CrossRef]
112. Nguyen, D.K.; Jang, C.H. An acetylcholinesterase-based biosensor for the detection of pesticides using liquid crystals confined in microcapillaries. *Colloids Surf. B Biointerfaces* **2021**, *200*, 111587. [CrossRef]
113. Singh, S.K.; Nandi, R.; Mishra, K.; Singh, H.K.; Singh, R.K.; Singh, B. Liquid crystal based sensor system for the real time detection of mercuric ions in water using amphiphilic dithiocarbamate. *Sens. Actuat. B-Chem.* **2016**, *226*, 381–387. [CrossRef]
114. Prévôt, M.E.; Nemati, A.; Cull, T.R.; Hegmann, E.; Hegmann, T. A Zero-Power Optical, ppt- to ppm-Level Toxic Gas and Vapor Sensor with Image, Text, and Analytical Capabilities. *Adv. Mater. Technol.* **2020**, *5*, 2000058. [CrossRef]
115. Ailincai, D.; Pamfil, D.; Marin, L. Multiple bio-responsive polymer dispersed liquid crystal composites for sensing applications. *J. Mol. Liq.* **2018**, *272*, 572–582. [CrossRef]
116. Popov, P.; Mann, E.K.; Jakli, A. Thermotropic liquid crystal films for biosensors and beyond. *J. Mater. Chem. B* **2017**, *5*, 5061–5078. [CrossRef]
117. Seo, J.M.; Khan, W.; Park, S.Y. Protein detection using aqueous/LC interfaces decorated with a novel polyacrylic acid block liquid crystalline polymer. *Soft Matter* **2012**, *8*, 198–203. [CrossRef]
118. Li, L.; Bai, H.; Dong, X.; Jiang, Y.; Li, Q.; Wang, Q.; Yuan, N.; Ding, J. Flexible Capacitive Sensors Based on Liquid Crystal Elastomer. *Langmuir* **2023**, *39*, 12412–12419. [CrossRef] [PubMed]
119. Park, H.; Lee, H.J.; Ahn, H.; Han, W.C.; Yun, H.S.; Choi, Y.S.; Kim, D.S.; Yoon, D.K. Mechanochromic Palettes of Cholesteric Liquid Crystal Elastomers for Visual Signaling. *Adv. Opt. Mater.* **2024**, *12*, 2400266. [CrossRef]
120. Fallah-Darrehchi, M.; Zahedi, P.; Harirchi, P.; Abdouss, M. Performance of Liquid Crystalline Elastomers on Biological Cell Response: A Review. *ACS Appl. Polym. Mater.* **2023**, *5*, 1076–1091. [CrossRef]
121. Shimatani, A.; Hoshi, M.; Oebisu, N.; Iwai, T.; Takada, N.; Nakamura, H. Clinical significance of thermal detection of soft-tissue tumors. *Int. J. Clin. Oncol.* **2020**, *25*, 1418–1424. [CrossRef]
122. Deng, F.; Tang, Q.; Zeng, G.; Wu, H.; Zhang, N.; Zhong, N. Effectiveness of digital infrared thermal imaging in detecting lower extremity deep venous thrombosis. *Med. Phys.* **2015**, *42*, 2242–2248. [CrossRef]
123. Fierheller, M.; Sibbald, R.G. A clinical investigation into the relationship between increased periwound skin temperature and local wound infection in patients with chronic leg ulcers. *Adv. Skin Wound Care* **2010**, *23*, 369–379; quiz 380–361. [CrossRef]
124. Li, W.; Khan, M.; Lin, L.; Zhang, Q.; Feng, S.; Wu, Z.; Lin, J. Monitoring H_2O_2 on the Surface of Single Cells with Liquid Crystal Elastomer Microspheres. *Angew. Chem.* **2020**, *132*, 9368–9373. [CrossRef]
125. Velasco-Abadia, A.; White, T.J.; Schwartz, D.K.; Kaar, J.L. 4D Cumulative Dose Sensing of Malathion Using a Biocatalytic Liquid Crystal Elastomer with Chemical Memory. *Sens. Actuators B Chem.* **2024**, *400*, 134877. [CrossRef]
126. Davidson, E.C.; Kotikian, A.; Li, S.; Aizenberg, J.; Lewis, J.A. 3D Printable and Reconfigurable Liquid Crystal Elastomers with Light-Induced Shape Memory via Dynamic Bond Exchange. *Adv. Mater.* **2020**, *32*, e1905682. [CrossRef]
127. Kotikian, A.; Morales, J.M.; Lu, A.; Mueller, J.; Davidson, Z.S.; Boley, J.W.; Lewis, J.A. Innervated, Self-Sensing Liquid Crystal Elastomer Actuators with Closed Loop Control. *Adv. Mater.* **2021**, *33*, e2101814. [CrossRef] [PubMed]
128. Saed, M.O.; Ambulo, C.P.; Kim, H.; De, R.; Raval, V.; Searles, K.; Siddiqui, D.A.; Cue, J.M.O.; Stefan, M.C.; Shankar, M.R.; et al. Molecularly-Engineered, 4D-Printed Liquid Crystal Elastomer Actuators. *Adv. Funct. Mater.* **2018**, *29*, 1806412. [CrossRef]

129. Lu, X.; Ambulo, C.P.; Wang, S.; Rivera-Tarazona, L.K.; Kim, H.; Searles, K.; Ware, T.H. 4D-Printing of Photoswitchable Actuators. *Angew. Chem. Int. Ed. Engl.* **2021**, *60*, 5536–5543. [CrossRef] [PubMed]

130. Rivera-Tarazona, L.K.; Shukla, T.; Singh, K.A.; Gaharwar, A.K.; Campbell, Z.T.; Ware, T.H. 4D Printing of Engineered Living Materials. *Adv. Funct. Mater.* **2021**, *32*, 2106843. [CrossRef]

131. McDougall, L.; Herman, J.; Huntley, E.; Leguizamon, S.; Cook, A.; White, T.; Kaehr, B.; Roach, D.J. Free-Form Liquid Crystal Elastomers via Embedded 4D Printing. *ACS Appl. Mater. Interfaces* **2023**, *15*, 58897–58904. [CrossRef]

132. Ambulo, C.P.; Tasmim, S.; Wang, S.; Abdelrahman, M.K.; Zimmern, P.E.; Ware, T.H. Processing advances in liquid crystal elastomers provide a path to biomedical applications. *J. Appl. Phys.* **2020**, *128*, 140901. [CrossRef]

133. Zhang, Z.; Yang, X.; Zhao, Y.; Ye, F.; Shang, L. Liquid Crystal Materials for Biomedical Applications. *Adv. Mater.* **2023**, *35*, e2300220. [CrossRef]

134. Barnes, M.; Cetinkaya, S.; Ajnsztajn, A.; Verduzco, R. Understanding the effect of liquid crystal content on the phase behavior and mechanical properties of liquid crystal elastomers. *Soft Matter* **2022**, *18*, 5074–5081. [CrossRef]

135. Ustunel, S.; Pandya, H.; Prevot, M.E.; Pegorin, G.; Shiralipour, F.; Paul, R.; Clements, R.J.; Khabaz, F.; Hegmann, E. A Molecular Rheology Dynamics Study on 3D Printing of Liquid Crystal Elastomers. *Macromol. Rapid Commun.* **2024**, *45*, e2300717. [CrossRef]

136. Zhang, W.; Nan, Y.; Wu, Z.; Shen, Y.; Luo, D. Photothermal-Driven Liquid Crystal Elastomers: Materials, Alignment and Applications. *Molecules* **2022**, *27*, 4330. [CrossRef]

137. Ford, M.J.; Ambulo, C.P.; Kent, T.A.; Markvicka, E.J.; Pan, C.; Malen, J.; Ware, T.H.; Majidi, C. A multifunctional shape-morphing elastomer with liquid metal inclusions. *Proc. Natl. Acad. Sci. USA* **2019**, *116*, 21438–21444. [CrossRef]

138. Zhang, J.; Guo, Y.; Hu, W.; Soon, R.H.; Davidson, Z.S.; Sitti, M. Liquid Crystal Elastomer-Based Magnetic Composite Films for Reconfigurable Shape-Morphing Soft Miniature Machines. *Adv. Mater.* **2021**, *33*, e2006191. [CrossRef] [PubMed]

139. Xia, Y.; Mu, T.; Liu, Y.; Leng, J. Harnessing the power of carbon fiber reinforced liquid crystal elastomer composites for high-performance aerospace materials: A comprehensive investigation on reversible transformation and shape memory deformation. *Compos. Part A Appl. Sci. Manuf.* **2024**, *177*, 107943. [CrossRef]

140. Mistry, D.; Connell, S.D.; Mickthwaite, S.L.; Morgan, P.B.; Clamp, J.H.; Gleeson, H.F. Coincident molecular auxeticity and negative order parameter in a liquid crystal elastomer. *Nat. Commun.* **2018**, *9*, 5095. [CrossRef] [PubMed]

141. Cooper, E.J.; Reynolds, M.; Raistrick, T.; Berrow, S.R.; Jull, E.I.L.; Reshetnyak, V.; Mistry, D.; Gleeson, H.F. Controlling the optical properties of transparent auxetic liquid crystal elastomers. *Macromolecules* **2024**, *57*, 2030–2038. [CrossRef] [PubMed]

142. Mazaev, A.V.; Ajeneza, O.; Shitikova, M.V. Auxetic materials: Classification, mechanical properties and applications. *IOP Conf. Ser. Mater. Sci. Eng.* **2020**, *747*, 012008. [CrossRef]

143. Ebrahimi, M.S.; Noruzi, M.; Hamzehei, R.; Etemadi, E.; Hashemi, R. Revolutionary auxetic intravascular medical stents for angioplasty applications. *Mater. Des.* **2023**, *235*, 112393. [CrossRef]

144. Amigo-Melchior, A.; Finkelmann, H. A concept for bifocal contact- or intraocular lenses: Liquid single crystal hydrogels ("LSCH"). *Polym. Adv. Technol.* **2002**, *13*, 363–369. [CrossRef]

145. Foster, L.; Peketi, P.; Allen, T.; Senior, T.; Duncan, O.; Alderson, A. Application of auxetic foam in sports helmets. *Appl. Sci.* **2018**, *8*, 354. [CrossRef]